Per. Mineral. (2003), *72*, SPECIAL ISSUE: *Eurocarb*, **223-251** http://go.to/permin

PERIODICO di MINERALOGIA
established in 1930

An International Journal of
MINERALOGY, CRYSTALLOGRAPHY, GEOCHEMISTRY, ORE DEPOSITS, PETROLOGY, VOLCANOLOGY
and applied topics on *Environment, Archaeometry* and *Cultural Heritage*

Leucite melilitolites in Italy: genetic aspects and relationships with associated alkaline rocks and carbonatites

FRANCESCO STOPPA[1]*, ALDO CUNDARI[2], GIANLUIGI ROSATELLI[1] and ALAN R.WOOLLEY[3]

[1] Università G. d'Annunzio, Dipartimento di Scienze della Terra, Via dei Vestini, 30 - 66100-Chieti Scalo (CH) Italy
[2] Università Federico II, Napoli
[3] Department of Mineralogy, The Natural History Museum, London, U.K.

ABSTRACT. — New bulk-rock and mineral data on leucite melilitolite from Italy are presented, compared and discussed in terms of their parageneses, petrological significance and petrogenesis. Melilitolite is an intrusive assemblage with more than 10% modal melilite. Leucite-bearing melilitolite (italite?) is so far only known from Italy, contains about 30vol.% melilite and up to 25vol.% leucite. Other felsic constituents are kalsilite, nepheline and haüyne. It occurs as dykes, sills and a plug in the kamafugite –carbonatite suite forming the Pleistocene Intra-mountain Ultra-alkaline Province (IUP). In addition, ejecta of melilite-bearing, leucite and/or kalsilite clinopyroxenite as well as foid-free ultramelilitolite occur in alkaline, high-K volcanics from the Roman Comagmatic Region (RR). Essential mineral chemistry shows that the ubiquitous clinopyroxene signals crystallization from peralkaline liquids in its T site configuration but also, notably in RR ejecta, crystallization from metaluminous liquids.

Melilite is characterised by a high gehlenite composition, similar to the melilite from a Ugandan (Fort Portal) calcite carbonatite lava. All IUP leucite melilitolites yielded lower Mg# and Cr+Ni, relative to the associated melilitites, and their parental liquid is residual with respect to the initial melilititic melt. The melilitolite liquid was highly enriched in CaO and alkalis and depleted in Al_2O_3 (agpaitic index > 0.9). High CaO and association with carbonatites have been proved to be unrelated to sedimentary limestones, but are linked to $CaCO_3$ decoupling and reaction with the silicate fraction to form melilitolites and/or, by early $CaCO_3$ immiscibility at high temperature, to form carbonatites. The occurrence of carbonate in globules, ocelli, and patches in melilitolite groundmass, is interpreted to have resulted from limited, late-stage immiscibility at relatively low temperature (670-800°C) and low pressure (<1 kb), favoured by residual fluid concentrations. Based on stratigraphic and structural observations, IUP melilitolites represent a final event in the related volcanic activity, inferred to have occurred as a slow, sub-volcanic intrusion which mechanically deformed the pre-existing rocks (brecciation, dragging and warping). IUP melilitolites and RR ejecta yielded a distinct mineral chemistry and modal abundance which reflect their initial peralkaline and metaluminous nature, respectively. This distinction is sharp for IUP melilitolites, but is blurred for RR ejecta. This may be due to the absence at the surface of a carbonatite component, non-essential modal melilite and essential feldspars in the RR assemblages. It is inferred that kamafugites may have originated from a deeper source, under a thicker lithosphere and lower heat flow, reflecting their close association with carbonatite, in contrast with conditions that prevailed for the generation of the much more abundant RR plagio-leucitite melts.

RIASSUNTO. — In questo lavoro vengono presentati nuovi dati mineralogici e composizionali sulle melilitoliti a leucite (italite?) Italiane. Tali dati sono messi a confronto tra loro e discussi in modo da definire la paragenesi e la petrogenesi di queste rocce. Le melilitoliti sono rocce subvulcaniche che contengono almeno il 10% di melilite. Le melilitoliti a leucite sono peculiari dell'Italia e contengono tipicamente il 30% di melilite e fino al 25% di

* Corresponding author, E-mail: fstoppa@unich.it

leucite. Altre componenti felsiche sono la kalsilite la nefelina e l'haüyna. Le melilitoliti si rinvengono sotto forma di dicchi, filoni strato e riempimento di condotti eruttivi e sono associate a rocce kamafugitiche (kalsilite melilitite) nella Provincia Intramontana Ultralcalina (IUP). Inoltre, una serie d'ejecta con melilite, per lo più leucite o kalsilite clinopirosseniti, ma anche ultramelilitoliti prive di foidi si ritrova nelle rocce alte in potassio della Provincia Comagmatica Romana (RR).

Il chimismo dei minerali essenziali mostra che il clinopirosseno, onnipresente in queste rocce, indica che essi hanno cristallizzato da liquidi peralcalini ma anche, specie nella RR da liquidi metalluminosi. La melilite contiene una notevole frazione molare di tipo gehelentico, non diversa da quella della melilite nelle carbonatiti di Fort Portal in Uganda, area tipica per le kamafugiti. Tutte le melilitoliti hanno un Mg# e Cr+Ni più basso rispetto alle associate melilititi, dando indicazione che esse siano termini più evoluti rispetto al magma melilititico capostipite. Il liquido da hanno cristallizzato le melilitoliti rappresenta un termine kamafugitico arricchito in calcio e in alcali, impoverito, viceversa, in alluminio (indice agpaitico = 0,9) e in elementi compatibili. L'elevato contenuto in calcio e l'associazione con carbonatiti, chiaramente non deriva da assimilazione di carbonato sedimentario, ma è legato alla dissociazione di carbonato igneo e alla ricombinazione del Ca con la frazione silicatica nella genesi delle melilitoliti a bassa pressione oppure a immiscibilità tra kamafugite e carbonatite a più alte pressioni. Tuttavia la presenza di ocelli, globuli di carbonato nella massa essenziale delle melilitoliti indica che una fase d'immiscibilità minore si è verificata anche a bassa pressione e bassa temperatura (670-800°C). In base alle loro caratteristiche chimiche e alla posizione stratigrafica, si può affermare che le melilitoliti rappresentino un episodio tardo-magmatico avvenuto lentamente e in condizioni sub-vulcaniche con conseguente deformazione meccanica delle rocce preesistenti (brecciatura, trascinamento, sollevamento).

Gli ejecta della RR hanno una diversa paragenesi e composizione mineralogica, che riflette la natura metalluminosa del liquido capostipite. Una possibile ragione di questa differenza potrebbe consistere nell'assenza di una componente carbonatitica nel magmatismo della RR e della contemporanea cristallizzazione di plagioclasio, assente nelle rocce kamafugitiche. Se ne deduce che le kalsilite olivin melilititi (kamafugiti), le melilitoliti e le carbonatiti possono essersi generate ad una profondità notevolmente maggiore, sotto una litosfera più spessa e con gradiente geotermico debole, riflettendo quindi bassi gradi di fusione parziale in contrasto con le condizioni prevalenti per la formazione delle molto più voluminose plagio leucititi della RR.

KEY WORDS: *Melilitolite, kamafugite, carbonatite, petrography, mineral and bulk-rock chemistry, petrogenesis.*

INTRODUCTION

Melilitolite is an intrusive rock which contains modal melilite>10% by volume. Melilitolites with modal melilite >65vol%, are called ultra-melilitolites (Dunworth and Bell, 1998). Melilitolite nomenclature rests on modal composition owing to its holocrystalline nature. The most abundant mineral constituent defines the terms afrikandite (magnetite-perovskite), turjaite (nepheline), okaite (haüyne), uncompahgrite (clinopyroxene) and kugdite (olivine). Leucite melilitolites (italite?) are only known from Italy and this paper reviews the significance of their occurrence. Italian leucite melilitolites show a Mafic Index= 90-56, implying a subordinate amount of foids. The investigated specimens are devoid of olivine and other mafic phases, i.e clinopyroxene, phlogopite, wollastonite, calcite; Ti-magnetite, cuspidine and götzenite may be important. Notably, Italian leucite melilitolites are closely associated in the field with carbonatites and kamafugites, which are considered co-magmatic (Stoppa, 2003). Therefore, their petrogenesis needs to be investigated in that context in order to establish their genetic relationships and related tectonic environment(s).

In this paper, new mineral and bulk-rock data on Italian leucite melilitolites are given with a view to exploring possible genetic relationships with coeval, regionally associated rock types.

FIELD OCCURRENCE

Two leucite melilitolite dykes and a leucite melilitolite plug occur as subvolcanic bodies in the Pleistocene Intra-mountain Ultra-alkaline

Province (IUP, Lavecchia and Stoppa, 1996; Lavecchia and Boncio, 2000; Lavecchia and Creati, 2002) and its most southerly extension, at Mt Vulture (Fig. 1). The IUP is distinct from the Roman Comagmatic Region (RR), dominated by plagio-leucitites, as it mainly consists of Ca-carbonatites and kamafugites (Stoppa and Woolley, 1997). RR melilite-bearing clinopyroxenite and ultra-melititolite rocks have been reported only as ejecta (Federico *et al.*, 1994; Schingaro *et al.*, 2001). A sill of leucite melilitolite composition occurs at San Venanzo, Umbria, central Italy (Fig. 1). The sill is formed by a coarse-grained to pegmatoid rock 1 m thick at the base of a kamafugite lava. This lava is brecciated and intruded by a melilitolite dykelet swarm that originated from the sill.

A plug-like body occurring at Colle Fabbri (Fig. 1) in the Spoleto region of central Italy was first described by Stoppa (1988). It consists of a holocrystalline, medium-grained, equigranular, light grey rock exposed for about 500 m^2, but traceable for about 2 km along a normal fault. It clearly cross-cuts country rocks and an explosion breccia.

A third melilitolite occurrence is from the Vulture area (southern Italy). Here, a 4 m thick dyke cuts phonolite, foidite pyroclastics and lavas and is associated with melilititic rocks.

In all the above occurrences melilite-bearing subvolcanic rocks and lavas form minor bodies, which are subordinate to associated pyroclastic rocks and appear to be related to late-stage volcanic activity.

In the RR, the Villa Senni locality of the Alban Hills is famous for the occurrence of Italite, a leucite melilitolite having 50-60vol% leucite, 18-23vol% melilite and 16-20vol% clinopyroxene plus Ti-magnetite, calcite, apatite (Washington, 1923). However, the investigated ejecta (blocks) rarely contain melilite and are mostly leucite or kalsilite-clinopyroxenites. They occur in the Alban Hills (south of Rome) and Montefiascone (north of Rome) volcanoes (Federico and Gianfagna, 1982; Federico *et al.*, 1994; Di Battistini *et al.*, 1998). Foid-free ultra-melilitolite, mainly composed of melilite plus essential spinel is represented by ejecta in leucite-phonolite

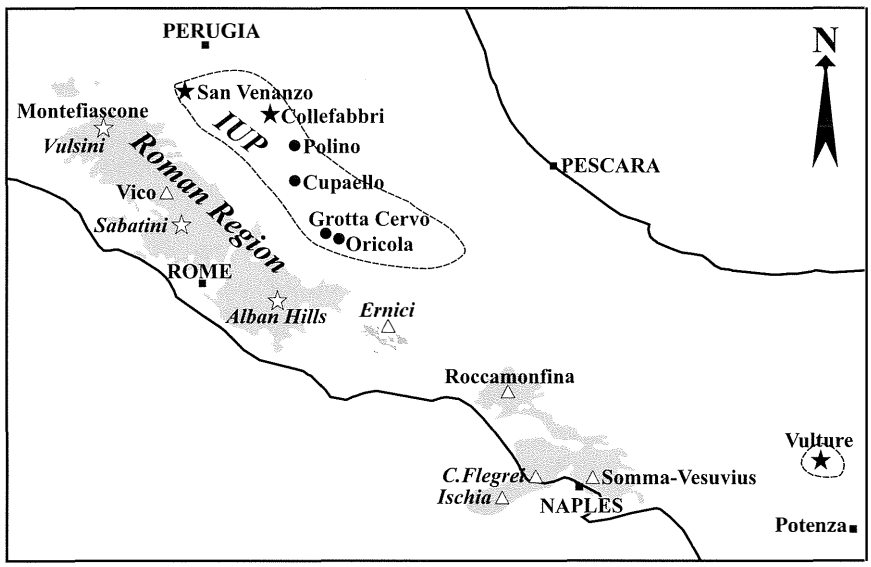

Fig. 1 – Sketch map showing the Roman Region, Intra-mountain Ultra-alkaline Province and melilitolite localities. Symbol key: solid stars: *in situ* melilitolites; Open stars: ejecta.

pyroclastic flows from the Sabatini volcanic complex (north of Rome) (Schingaro *et al.*, 2001). Some of these ejecta are probably fragments of hypabyssal or plutonic rocks which derived from older magmatic activity. However, the nature of these ejecta needs to be investigated in the context of the Italian melilitolite group, even if their modal composition, texture and occurrence appear, generally, to be very different from those of IUP leucite melilitolites.

PETROGRAPHY

San Venanzo melilitolite (SV)

The calcite-leucite-melilitolite of Pian di Celle (San Venanzo) has been famous for over a century, and was previously called pegmatoid venanzite (Gallo *et al.*, 1984). It contains tabular melilite up to 5 cm long, nepheline intergrowths associated with coarse-grained, intergranular, twinned leucite, nepheline and kalsilite as essential minerals (Plate 1: photo A; Plate 2: photos 1 and 2; Table 1). The interstices between these phases are filled with a fine-grained groundmass composed of F-apatite, F-phlogopite, clinopyroxene, Zr-cuspidine, götzenite, khibinskite, pyrrhotite, Co-Ni-westerveldite, bartonite, wollastonite and brown or green glass (Sharygin *et al.*, 1996; Stoppa *et al.*, 1997). Olivine and monticellite also occur (Table 7). The interstitial material commonly contains carbonate ocelli with high Sr, Ba and REE (Stoppa and Woolley, 1997).

Colle Fabbri melilitolite (CF).

Originally called euremite by Stoppa (1988), this rock forms a plug and is modally a leucite-wollastonite melilitolite (Table 1), according to Dunworth and Bell (1998). It is dominantly medium-grained and equigranular, but fine-grained at the margins with calcite-zeolite filled ocelli (Plate 1, photo B). It is composed of melilite euhedra, up to 5mm across, poikilitically enclosing wollastonite prisms, sometimes in optical continuity (Plate 2: photos C). Melilite shows anomalous blue-grey interference colours and a yellow rim (Plate 2: photo D). It often displays peg structure and is intergrown with foids (leucite and minor kalsilite) (Plate 2: photo E). Glass inclusions occur in wollastonite. Leucite is the main intergranular constituent together with Ti-magnetite. Accessory phases are brown-red garnet (schorlomite) and apatite. Anorthite is common and occurs in patches (Plate 2: photo F). The order of crystallization, from textural relationships, is wollastonite, melilite, anorthite, Ti-magnetite, schorlomite and leucite. Quench clinopyroxene is present at chilled margins where melilite is rare and mostly replaced by anorthite. Late-stage calcite and zeolite are uncommon but very abundant in the melilitolite chilled margins. Locally, a glassy facies with tridymite and cordierite at the contact with the country rocks indicates a high magmatic temperature.

Pietra della Scimmia (PS).

This is a medium-grained leucite melilitolite, representing one of the numerous melilitite occurrences from Vulture (Fig. 1) which form dykes, lavas and tuff (Stoppa and Principe, 1998; Melluso *et al.*, 1996). The rock is composed of large (up to 5 mm. across), tabular, euhedral melilite with clinopyroxene inclusions along cleavages. It never displays peg structure. Melilite laths exhibit a weak flow structure and may show some optical continuity. Rounded melilite with concentric inclusions, as well as patchy melilite also occur. Other phenocrysts are corroded clinopyroxene with oscillatory zoning and a thin reaction rim, and rare haüyne. The groundmass is composed of melilite, leucite, haüyne, nepheline, clinopyroxene, Ti-magnetite, garnet, sphene, perovskite and apatite (Table 1). Garnet micro-phenocrysts are slightly turbid, yellow-brownish, subhedral to anhedral, birefringent and twinned. It is mainly a melanite with moderate amounts of molar pyrope (up to 25%) and TiO_2 up to 8wt.%. Apatite occurs as small anhedral to euhedral

Plate 1 – A. Pian di Celle (San Venanzo-Umbria) kalsilite-leucite melilitolite hand specimen. Note elongate, irregular melilite crystals and rounded leucite in a finer groundmass with calcite ocelli; B: Colle Fabbri (Spoleto, Umbria), leucite-wollastonite melilitolite hand specimen. Note small calcite-zeolite ocelli. C: Preta della Scimmia (Mt. Vulture-Lucania), haüyne-leucite melilitolite hand specimen. Note melilite and clinopyroxene prisms, clear and darker, respectively, in a fine-grained groundmass.

groundmass prisms and also as acicular crystals. Honey yellow, clear perovskite forms euhedra, with characteristic internal reflections (Table 10). Calcite forms small, intergranular, turbid patches in the groundmass. Rare celsian has been detected by EMP (Table 10).

Alban Hills (AH)

Federico *et al.*, (1994) reviewed a variety of ultramafic ejecta, ranging from spinel-phlogopite-clinopyroxenite, leucite-clinopyroxenite to kalsilite-clinopyroxenite from the Alban Hills volcanic complex (Fig. 1). Melilite was not reported from the ultramafic assemblages and other mafic or felsic holocrystalline xenoliths. However, Aurisicchio and Federico (1985) and Federico and Gianfagna (1982) described melilite associated with, in order of frequency, phlogopite, clinopyroxene, magnetite, kaliophylite, melanite garnet, leucite, kalsilite, haüyne, apatite, perovskite and lesser olivine, amphibole and nepheline (Table 7-9). Modal melilite is subordinate to clinopyroxene, phlogopite, melanite and leucite. A typical specimen is represented by kalsilite clinopyroxenite, in which the coexisting phases are clinopyroxene, kalsilite, leucite, magnetite, garnet, phlogopite, apatite, and very rare melilite. Based on essential mineralogy these ejecta are kalsilite or leucite clinopyroxenite and not melilitolite. Ejecta from Colle Cimino, near Marino, were also investigated, i.e. AH/25, AH/26 and AH/3 (i.e. KLT of Federico *et al.* 1994). They consist of leucite clinopyroxenite and kalsilite clinopyroxenite, respectively (Table 1). Leucite clinopyroxenite (sample AH/25, Table 1, Plate 3: photos A and B) shows inequigranular texture with areas of coarse granularity with large twinned leucite and clinopyroxene in a fine-grained, equigranular clinopyroxene matrix with intergranular leucite. Kalsilite clinopyroxenite (sample AH/3, Table 1, Plate 3: Photos C and D) shows inequigranular texture with large patchy kalsilite hosting anhedral clinopyroxene and garnet. Clinopyroxene shows nuclei not in optical continuity with the rims, stress twinning

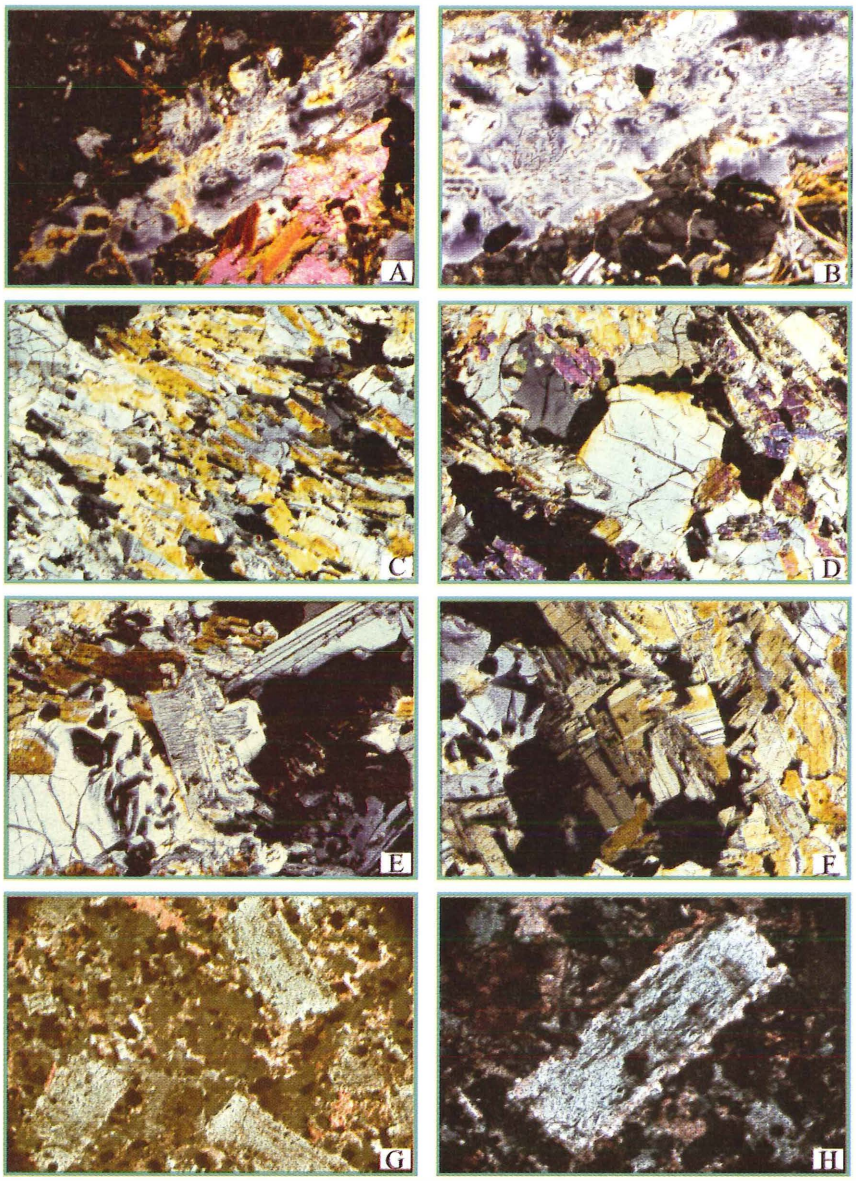

Plate 2 – Photos A and B: Pian di Celle (San Venanzo, Umbria) kalsilite-leucite melilitolite, 2x and 5x, crossed polars. A: Blue-yellow pegmatoid melilite with irregular, elongate shape, surrounded by large round twinned leucite, and clinopyroxene and mica flakes. B: Melilite with nepheline inclusions associated with coarse-grained, intergranular, twinned leucite and carbonate. Photos C. D, E and F, Colle Fabbri leucite-wollastonite melilitolite, C is 5x, the 1D-F 10x, crossed polarized light. C: Melilite euhedra, poikilitically enclosing wollastonite prisms in optical continuity; D: Melilite with anomalous blue-grey interference colours and a yellow rim; leucite is at extinction. Photo E: Peg structure in melilite, at centre, and symplectite-like intergrown with foids, at left. Photo F: Anorthite with leucite (at extinction). Photos G-H: Pietra della Scimmia, haüyne-wollastonite melilitolite; 5x and 10x, crossed polars. Large laths of melilite in fine grained groundmass of melilite, leucite, clinopyroxene, Ti-magnetite, nepheline etc. Melilite lath with clinopyroxene inclusions along cleavage.

TABLE 1

Modal composition of Intra-mountain Ultra-alkaline Province leucite melilitolite and melilite-bearing ejecta from the Roman Region. Modal abundances calculated by about 1000 analytical points per section. Reconnaissance analyses by Hitachi SEM-EDS scanning.

occurrence	San Venanzo	San Venanzo	Colle-Fabbri	Pietra della Scimmia (Vulture)	Alban Hills	Alban Hills	Anguillara Sabina (Sabatini)	Monte-fiascone (Vulsini)
sample	SV	SV[1]	CF	PS	AH/25	AH/3	AS[2]	MF/9
nepheline	9.5	7	-	9.4	-	x	-	-
kalsilite	6.8		x	-	-	35.5	-	8.38
leucite	19.3	25	9.12	25.1	20.6	2.5	-	1.53
haüyne	-	-	-	10	2.07	-	-	x
anorthite	-	-	6.1	-	-	-	-	-
melilite	25.7	28	32	33.7	x	x	73	x
clinopyroxene	7	5	x	6.75	74.2	50.7	-	84
wollastonite	-	-	47.9	-	-	-	-	x
olivine	x	2	-	-	x	-	-	x
mica	8.7	9	-	x	-	2.4	-	x
garnet	-	-	1.01	0.61	1.38	6.7	x	x
magnetite	10.4	4	1.01	1.01	x	-	-	x
spinel	-	-	-	-	-	1.2	15	-
calcite	4.2	12	x	1.84	-	-	-	-
perovskite	x	x	-	1.43	-	-	-	-
apatite	2.8	2	1.01	1.01	0.69	0.8	-	0.3
K-zeolite	1.9	x	1.77	x	0.6	-	-	4.5
Zr-cuspidine	2.8	3	-	-	-	-	-	-
Ti- götzenite	1.9	-	-	-	-	-	-	-

x <0.5%, - not detected, [1] Stoppa *et al.* (1997); [2] Schingaro *et al.* (2001)

and mosaic texture. Granoblastic layers with a fine mosaic texture crosscut the rock. Absence of leucite and presence of strain features suggest a higher pressure origin with respect to AH/25.

Sabatini (SAB)

Schingaro *et al.* (2001) described a holocrystalline block from Anguillara Sabazia, Sabatini Volcanic Complex, embedded in a pyroclastic flow (Fig. 1). This is a spinel ultra-melilitolite, with gehlenitic melilite exceeding 70% by volume plus pleonaste, rare kimzeyite garnet, pyrite and secondary barite (Table 1). Notably, it does not contain foids. The presence of kimzeyite garnet is noteworthy. Zr-garnet kimzeyite ($Ca_3Zr_2Fe_2SiO_{12}$) is a very rare mineral related to andradite ($Ca_3Fe_2Si_3O_{12}$) and schorlomite ($Ca_3Ti_2Fe_2SiO_{12}$) which are typical of RR ejecta and IUP rocks, respectively. In fact, Zr-schorlomite occurs in the Polino and Cupaello carbonatites (Lupini *et al.*, 1992; Stoppa and Cundari, 1995), which are regionally associated with CF and SV. Zr in these phases reflects high temperature as Ti-garnet and Zr-garnet form a complete solid solution in the range 1050-1200°C at low pressure (Ito and Frondel, 1967). At lower temperatures, Zr-cuspidine, reported from SV leucite melilitolite, is the main Zr carrier.

Montefiascone (MF)

Kalsilite-clinopyroxenite nodules occur in a tephrite-phonolite pyroclastic flow at the Montefiascone maar, Vulsini Volcanic Complex (Di Battistini *et al.*, 1998). Samples MF/5 and MF/9 were investigated from this locality. They are formed of dominant subhedral clinopyroxene, essential kalsilite plus leucite and very rare haüyne, melilite, garnet, mica, olivine and low-Ti magnetite (Table 7-8-9). Kalsilite clinopyroxenite has an intersertal-intergranular texture dominated by euhedral subhedral, long prisms of clinopyroxene with essential leucite and haüyne and much lesser andraditic garnet, olivine, apatite and small intergranular pools of glass and zeolites (Table 1, Plate 3: E and F). There is a clear textural indication of accumulation of clinopyroxene intergrowth with kalsilite indicating co-precipitation, and late intergranular leucite.

ESSENTIAL MINERALOGY

Pyroxene

Clinopyroxene analyses are given in Table 2. Clinopyroxene is subordinate (6-7vol%) in all IUP leucite melilitolites and at CF it occurs only in the chilled facies. In the RR ejecta clinopyroxene is dominant and consistently falls close to the Wo-En joint of the diopside field in the conventional pyroxene quadrilateral, with a clear trend towards Wo. The IUP pyroxene from melilitolite defines a variant trend towards Fs and Hd and is strongly enriched in Hd, which is dominant in the CF clinopyroxene rim compositions (Fig. 2). SV clinopyroxene contains appreciable Na. In terms of the T site occupancy, the RR clinopyroxene from ejecta follows a continuous trend on the Si-saturated side of the Si-Al diagram (Fig. 3a). The clinopyroxene from SV and AHB melilitolites also plots in the Al-undersaturated side of the (2-Si)=Al line, reflecting the peralkaline nature of the crystallizing liquid (i.e. Na+K>Al). The CF hedenbergitic rim composition is noteworthy in its undersaturated (Si+Al) T site, indicating an abrupt change of the crystallizing liquid to a strongly peralkaline composition (Fig. 3a). In addition, Stoppa *et al.* (1997), demonstrated that the evolution of melilitolitic melt resulted in the development of late-stage Fe-rich phases (westerveldite, pyrrhotite, bartonite, other sulphides and Fe-Ti-oxides). RR ejecta clinopyroxene give higher Mg# i.e. $100(Mg/Mg+Fe^{2+})$, and lower Ca# i.e. (Ca/Ca+Mg), which distinguish them from the more evolved IUP melilitolite clinopyroxene (Fig. 3b). RR clinopyroxene from RR ejecta is also distinct from the IUP leucite melilitolite analogue in containing relatively high $[Al]_{M1}$ and very low Ti and Fe (Figs 3c and d).

Melilite

Selected analyses of melilite are given in Table 3. Modal melilite is fairly constant at about 30%vol. in IUP leucite-melilitolites (Table 1), as well as the ratio melilite/clinopyroxene, indicating similar CaO/CO_2 saturation in these rocks. However, SV and PS melilite is distinct, relative to the analogues from CF and RR ejecta, in its low in Ca + Al vs high Fe + Si (Figs 4a and b), indicating that the latter two compositions are gehlenitic and that Fe-Åkermanite occurs at SV and PS.

The diagrams (Na+K)-Al-Mg and Fe-Al-Mg illustrate melilite relationships among and between IUP melilitolites and RR ejecta (Figs 5a and b). Within and between outcrop trends are consistent with the variation of the molar gehlenite/åkermanite ratio. Fe is low in CF samples and is considered mainly confined to Fe-Åk. In the CF samples, the molar fraction of Na-melilite is rather constant at about 6-8%, and molar åkermanite and gehlenite range between c. 20-30% and 60-70%, respectively, crystal cores being enriched in åkermanite. The alkali/Al ratio increases from 0.13 in CF, to 0.75 in PS, to 1.33 in SV. Alkali and Al consistently increase from core to rim. Alkali/Ca is about 0.25 for all occurrences, with Ca decreasing from core to rim. Molar fractions of Na-melilite and (Fe-åkermanite +

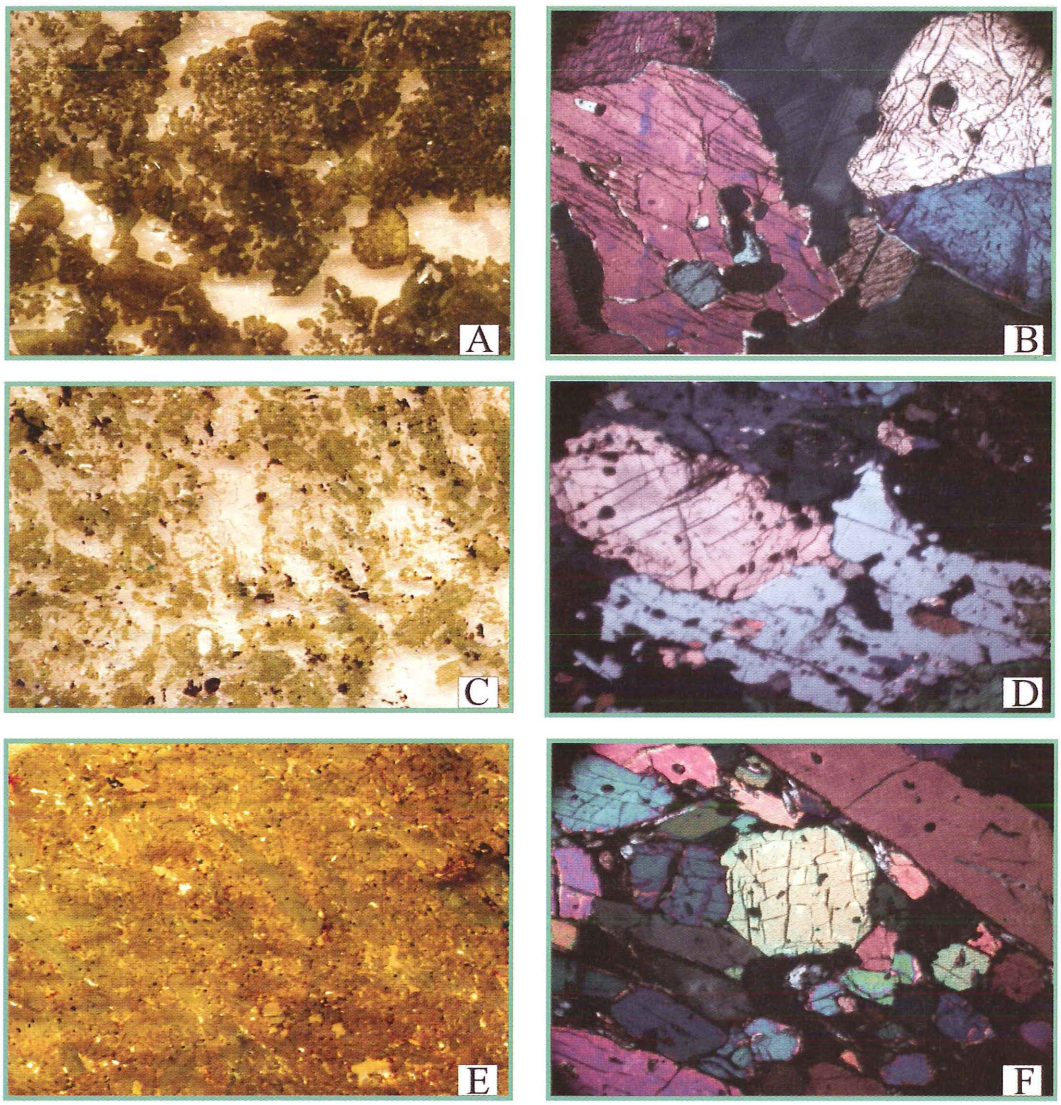

Plate 3 – Photos A and B: Leucite clinopyroxenite from Colle Cimino near Marino, Alban Hills, 3x, left reflected light, right transmitted polarised light. Photos C and D: Kalsilite clinopyroxenite, as above. Photos E and F: Kalsilite clinopyroxenite from Montefiascone Vulsini, as above.

Fe-gehlenite) are rather constant at about 6-8%. SrO, ZrO_2 and BaO do not seem to be distinctive and their sum is generally about 1wt.%. CF and RR ejecta are possibly related being characterised by an increasing Ca and Al contents with respect to Si and alkali (notably K), reflecting similar variations in the crystallising liquid.

Melilite in igneous rocks is generally believed to be a Na melilite-rich åkermanite (Yoder, 1973), whereas melilite in the Italian melilitolite rocks is characterised by a high

TABLE 2

Representative analyses of clinopyroxene.

	SV	SV	SV	CF a-core	CF a-rim	CF b-core	CF b-rim	CF Wo	CF Wo	PS	PS	AH/3	AH/3	AH/25	AH/25	MF9	MF9	MF5	MF5
SiO_2	52.75	52.05	52.16	48.86	43.25	47.69	44.45	51.36	51.74	43.05	41.11	50.66	50.80	46.92	48.31	50.02	49.90	53.57	49.69
TiO_2	0.82	1.73	1.88	0.42	0.97	0.56	0.95	0.04	0.05	2.57	4.68	0.60	0.57	1.02	0.88	0.52	0.61	0.26	0.68
Al_2O_3	0.53	0.47	0.61	4.92	5.36	5.06	5.03	0.05	0.04	8.18	9.39	3.11	2.03	6.26	5.15	4.30	4.36	1.89	5.53
FeO*	8.30	10.50	11.40	7.25	18.76	8.21	17.83	0.99	1.26	9.29	10.77	5.46	7.35	7.10	5.91	5.42	5.72	2.94	5.16
Fe_2O_3	0.73	1.33	nd	nd	nd	nd	nd	nd	nd	nd	nd	nd	nd	nd	nd	nd	nd	nd	nd
MnO	0.27	0.00	0.29	0.02	0.25	0.08	0.22	0.08	0.14	0.06	0.22	0.17	0.32	0.19	0.16	0.00	0.00	0.03	0.14
MgO	12.13	10.84	10.18	12.80	6.63	12.07	6.85	1.61	1.14	11.07	8.88	14.54	13.39	12.85	13.68	14.14	14.20	17.68	14.60
CaO	23.49	21.59	21.24	24.65	23.10	24.55	23.37	45.01	45.72	24.11	22.95	24.33	24.19	24.23	24.29	25.23	25.33	23.06	23.80
Na_2O	0.76	1.37	1.49	0.10	0.14	0.11	0.16	bdl	bdl	0.27	0.58	0.30	0.48	0.29	0.32	0.25	bdl	0.16	0.21
Total	99.78	99.88	99.25	99.02	98.46	98.33	98.86	99.15	100.08	98.60	98.58	99.17	99.13	98.86	98.70	99.88	100.12	99.59	99.81
Number of ions on the basis of 6 O																			
T Si	1.982	1.971	1.989	1.831	1.711	1.808	1.747	1.995	1.996	1.635	1.584	1.880	1.902	1.757	1.803	1.842	1.838	1.951	1.826
T Al	0.018	0.021	0.011	0.169	0.250	0.192	0.233	0.002	0.002	0.365	0.416	0.120	0.089	0.243	0.197	0.158	0.162	0.049	0.174
T Fe^{3+}	0.000	0.008	0.000	0.000	0.039	0.000	0.020	0.003	0.002	0.000	0.000	0.000	0.009	0.000	0.000	0.000	0.000	0.000	0.000
M1 Al	0.006	0.000	0.016	0.048	0.000	0.034	0.000	0.000	0.000	0.001	0.010	0.016	0.000	0.033	0.030	0.029	0.027	0.032	0.066
M1 Ti	0.023	0.049	0.054	0.012	0.029	0.016	0.028	0.001	0.001	0.073	0.136	0.017	0.016	0.029	0.025	0.014	0.017	0.007	0.019
M1 Fe^{3+}	0.021	0.023	0.000	0.104	0.241	0.134	0.208	0.003	0.001	0.235	0.177	0.093	0.101	0.173	0.140	0.117	0.100	0.014	0.084
M1 Fe^{2+}	0.261	0.316	0.351	0.121	0.339	0.127	0.359	0.027	0.038	0.060	0.167	0.071	0.121	0.048	0.044	0.050	0.076	0.000	0.031
M1 Mg	0.680	0.612	0.579	0.715	0.391	0.682	0.401	0.093	0.066	0.627	0.510	0.804	0.747	0.717	0.761	0.776	0.780	0.947	0.800
M2 Mg	0.000	0.000	0.000	0.000	0.000	0.000	0.000	0.000	0.000	0.000	0.000	0.000	0.000	0.000	0.000	0.000	0.000	0.013	0.000
M2 Fe^{2+}	0.000	0.023	0.013	0.002	0.002	0.000	0.000	0.000	0.000	0.000	0.002	0.006	0.000	0.001	0.000	0.000	0.000	0.075	0.043
M2 Mn	0.009	0.000	0.009	0.001	0.008	0.003	0.007	0.003	0.005	0.002	0.007	0.005	0.010	0.006	0.005	0.000	0.000	0.001	0.004
M2 Ca	0.946	0.876	0.868	0.990	0.979	0.997	0.984	1.873	1.890	0.981	0.947	0.967	0.970	0.972	0.971	0.996	1.000	0.900	0.937
M2 Na	0.055	0.101	0.110	0.007	0.011	0.008	0.012	-	-	0.020	0.043	0.022	0.035	0.021	0.023	0.018	-	0.011	0.015
Sum	4.000	4.000	4.000	4.000	4.000	4.000	4.000	4.000	4.001	4.000	4.000	4.000	4.000	4.000	4.000	4.000	4.000	4.000	4.000
Ca#	0.58	0.59	0.60	0.58	0.71	0.59	0.71	0.95	0.97	0.61	0.65	0.55	0.56	0.58	0.56	0.56	0.56	0.48	0.54
Mg#	0.72	0.64	0.61	0.85	0.53	0.84	0.53	0.78	0.63	0.91	0.75	0.91	0.86	0.94	0.95	0.94	0.91	0.93	0.92
End members																			
WO	49	47	48	51	49	51	50	94	94	52	52	50	50	51	51	51	51	46	49
EN	35	33	32	37	20	35	20	5	3	33	28	41	38	37	40	40	40	49	42
FS	15	20	20	12	31	14	30	2	2	16	20	9	12	12	10	9	9	5	9

*Total iron; Fe_2O_3 measured only in the SV samples. bdl – below detection limits (0.04 wt.%); nd – not determined; Fe^{3+}/Fe^{2+} ratio determined by charge balance.
Ca# = Ca/Ca+Mg; Mg# = Mg/Mg+Fe^{2+}. WO - Wollastonite; EN – Enstatite; FS – Ferrosilite.

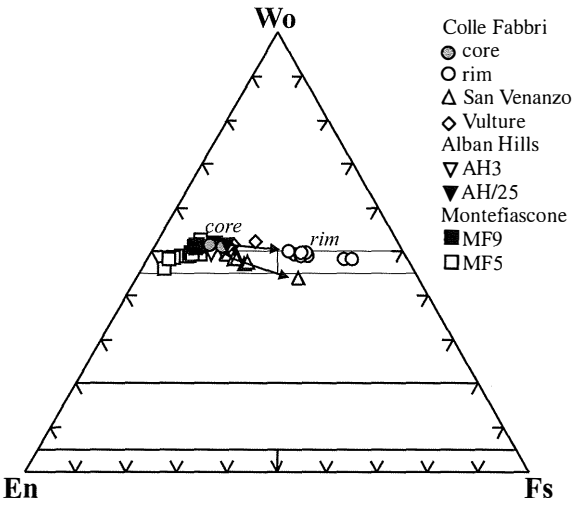

Fig. 2 – Conventional pyroxene quadrilateral showing clinopyroxene compositions of Intra-mountain Ultra-alkaline Province melilitolites and Roman Region ejecta

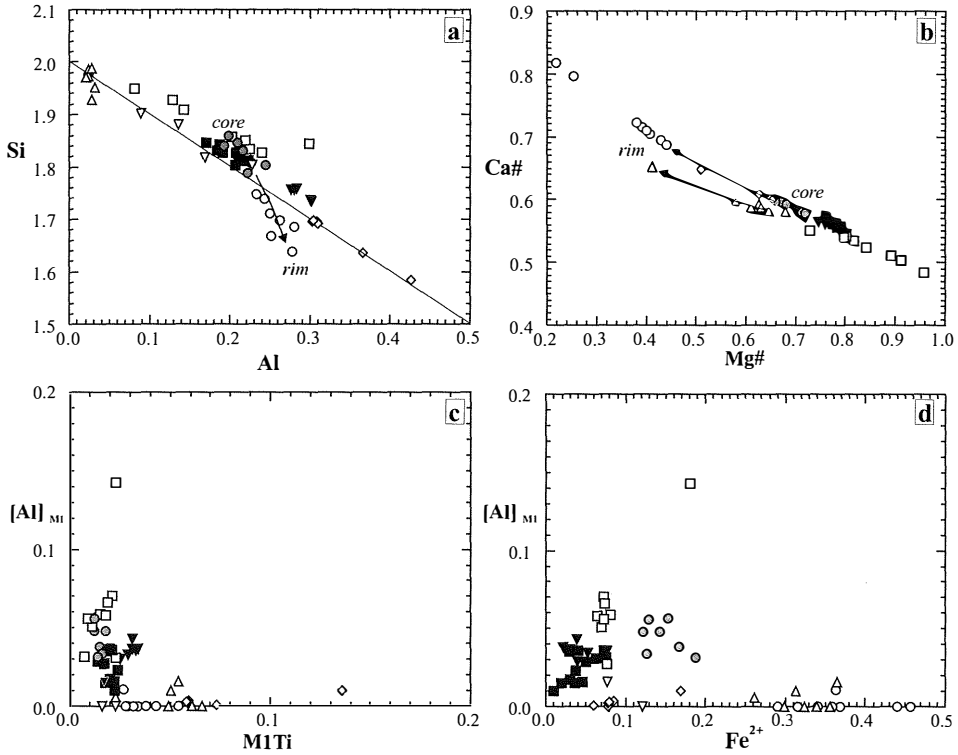

Fig. 3. a, b, c and d – Crystal chemistry of clinopyroxene from Intra-mountain Ultra-alkaline Province melilitolites compared with Roman Region ejecta analogues in terms of site occupancy and Mg# (Mg/Mg+Fe2+) and Ca# (Ca/Ca+Mg)

TABLE 3

Representative analyses of melilite.

location	SV 1	SV 2	CF 3	CF 4	AS** 5	PS 6	PS 7	MF9 8	MF9 9	AH25 10	AH25 11
SiO_2	43.24	43.28	32.97	36.41	35.67	44.57	43.89	40.04	41.45	38.87	40.04
Al_2O_3	3.83	3.41	19.99	14.84	13.51	7.63	6.51	6.15	5.35	3.82	6.94
TiO_2	bdl	0.15	bdl	bdl	0.04	bdl	bdl	1.68	0.59	1.01	1.63
FeO*	4.14	4.42	3.48	2.27	1.5	5.49	4.51	11.58	9.16	14.27	12.75
MgO	8.77	9.31	4.13	6.40	8.44	6.02	8.14	5.46	7.33	3.33	7.04
MnO	0.13	0.09	bdl	bdl	0.05	0.30	0.22	nd	nd	nd	nd
CaO	36.8	36.87	38.52	38.48	39.19	32.04	33.91	30.15	35.36	38.56	30.58
Na_2O	2.1	1.68	1.00	0.90	0.35	4.56	3.30	1.82	0.2	bdl	0.51
K_2O	0.29	0.32	0.52	0.50	0.07	0.22	0.17	2.93	0.36	0.49	0.23
Total	99.30	99.53	100.61	99.80	98.82	100.83	100.65	99.81	99.8	100.35	99.72
Number of ion son the basis of 14 O											
Si	3.995	3.992	3.019	3.334	3.296	4.017	3.937	3.807	3.865	3.765	3.753
Al	0.413	0.367	2.135	1.585	1.456	0.802	0.681	0.682	0.582	0.432	0.759
Ti	0.000	0.010	0.000	0.000	0.003	0.000	0.000	0.120	0.041	0.074	0.115
Fe	0.320	0.341	0.266	0.174	0.116	0.414	0.338	0.921	0.714	1.156	0.999
Mg	1.208	1.280	0.564	0.874	1.163	0.809	1.088	0.774	1.019	0.481	0.984
Mn	0.010	0.007	0.000	0.000	0.004	0.023	0.017	0.000	0.000	0.000	0.000
Ca	3.642	3.643	3.778	3.774	3.879	3.094	3.355	3.071	3.532	4.002	3.071
Na	0.376	0.300	0.177	0.160	0.063	0.797	0.574	0.336	0.036	0.000	0.093
K	0.034	0.038	0.061	0.058	0.008	0.025	0.019	0.355	0.043	0.061	0.028
Sum	9.998	9.978	10.001	9.959	9.987	9.981	10.009	10.067	9.833	9.969	9.801

* total iron. ** average of 5 analyses. bdl – below detection limits (0.04 wt.%). nd – not determined.

gehlenitic molecular fraction. However, at Mt.Vulture (Monticchio Lakes formation) melilite in the melilitite-carbonatite lapilli tuffs contains 33 mol% gehlenite (Stoppa and Principe, 1998).

It is noteworthy that gehlenitic melilite was reported from the calcite carbonatite lava from Fort Portal, Uganda (Barker and Nixon, 1989).

Wollastonite

Wollastonite is essential only in CF, but is reported from SV and possibly from some RR ejecta (Stoppani and Curti, 1982). Its composition is shown in Table 2.

Wollastonite is usually incorporated in diopside as solid solution in IUP melilitites. At CF wollastonite appears to be an early, high temperature liquidus mineral and shows a relatively high content of Mg and Fe, although Sr is virtually absent and BaO is less than 0.04 wt.%. Wollastonite is a common constituent of intrusive, ultramafic, melilite-bearing rocks, in assemblages of the ijolite series and in ultramafic lamprophyres, often associated with carbonatites, and occurs in carbonatites (Hogarth, 1989). Magmatic wollastonite occurs also in extrusive rocks e.g. the wollastonite phonolite from Fohberg (Kaiserstuhl) with up to 10% modal wollastonite (Albrect, 1981). High bulk-rock CaO, combined with high alkali and an agpaitic index of 0.9, clearly favour wollastonite crystallisation (Albrecht, 1981). These conditions are very similar to those inferred for the CF early crystallising liquid. In addition, mutual wollastonite, melilite, clinopyroxene textural relationships in

the quenched material of CF may be related to the limited stability of åkermanite in the presence of excess CO_2 at P<6kb, leading to the development of diopside, anorthite and calcite at relatively low, sub-solidus temperatures (Yoder, 1975).

Feldspathoids

The felsic components of IUP leucite melilitolites comprise ubiquitous leucite plus kalsilite, nepheline and haüyne. Representative analyses are given in Tables 4 to 6. Leucite and kalsilite yield highly variable relative abundances. Nepheline, an important essential mineral in IUP leucite melilitolites, occurs both in combination with haüyne or kalsilite (Table 1). Haüyne only occurs in PS samples but it is present in some IUP kamafugites, e.g. Grotta del Cervo (mela-foidite, Stoppa *et al.*, 2002), at Vulture and in RR ejecta. Foid compositions seem to be related to subsolidus breakdown and different retentivity of K and Na. Leucite, kalsilite, nepheline and haüyne are liquidus phases in IUP leucite melilitolites. Symplectite-like structures formed by melilite, nepheline and leucite (and possibly kalsilite) have been observed in SV and CF. Nepheline-kalsilite intergrowth structures are reported from RR samples (Aurisicchio and Federico, 1985).

The Si/Al ratio is slightly in excess of stoichiometry in leucite from RR ejecta and PS melilitolites and lower than stoichiometry in the CF and SV melilitolites (Table 4). IUP melilitolite leucite is also K-deficient with respect to RR analogues. On the other hand, Fe in SV and PS leucite is a factor of two higher than that in CF and RR leucite. While leucite is rare in deep-seated rocks, it should be noted

TABLE 4

Representative analyses of leucite

location	SV	SV	CF	CF	PS	PS	MF5	MF5	AH25	AH25
	1	2	3	4	5	6	7	8	9	10
SiO_2	53.52	53.38	54.49	53.73	55.24	54.77	55.40	55.32	53.75	53.75
Al_2O_3	23.20	23.30	23.54	23.56	23.22	22.86	23.19	22.86	23.48	23.48
TiO_2	bdl	bdl	bdl	bdl	bdl	0.26	0.04	0.07	bdl	bdl
Fe_2O_3*	0.62	0.61	0.27	0.32	0.58	0.76	0.33	0.33	0.31	0.31
MnO	bdl	bdl	bdl	bdl	bdl	bdl	0.05	0.05	bdl	bdl
Na_2O	0.20	bdl	bdl	bdl	bdl	bdl	0.32	0.21	0.39	0.39
K_2O	21.50	22.43	20.55	20.63	20.17	19.87	19.95	20.67	21.71	22.00
BaO	nd	nd	0.49	1.06	1.11	0.83	bdl	bdl	0.08	0.08
Total	99.04	99.72	99.34	99.30	100.32	99.35	99.29	99.54	99.72	100.01
Number of ion son the basis of 6 O										
Si	1.971	1.962	1.994	1.981	2.003	2.001	2.011	2.012	1.998	1.998
Ti	-	-	-	-	-	0.007	0.001	0.002	-	-
Al	0.997	0.999	1.015	1.024	0.992	0.984	0.992	0.980	0.985	0.985
Fe^{+3}	0.056	0.055	0.007	0.009	0.016	0.021	0.009	0.009	0.009	0.009
Mn	-	-	-	-	-	-	0.002	0.001	-	-
Na	0.014	-	-	-	-	-	0.022	0.015	0.028	0.028
K	1.010	1.052	0.941	0.947	0.933	0.926	0.924	0.959	0.996	0.996
Ba	-	-	0.007	0.015	0.016	0.012	-	-	0.001	0.001
Sum	4.047	4.068	3.965	3.976	3.960	3.952	3.961	3.979	4.017	4.017

* total iron. nd – not determined. bdl – below detection limits (0.04 wt.%).

TABLE 5

Representative analyses of nepheline and kalsilite

	kalsilite								nepheline			
location	SV 1	SV 2	SV 3	SV 4	MF9 5	MF9 6	MF9 7	MF9 8	SV 1	SV 2	PS 3	PS 4
SiO_2	37.82	38.46	39.30	39.57	38.79	38.05	37.91	38.08	42.00	40.93	42.88	42.54
Al_2O_3	28.59	29.28	29.47	30.05	32.00	31.37	31.25	31.56	30.34	29.13	33.07	33.09
FeO*	2.89	2.35	1.91	1.78	1.03	0.85	0.79	0.73	2.45	5.05	1.17	0.93
MgO	bdl	bdl	0.24	0.15	bdl	0.04	0.05	bdl	bdl	bdl	bdl	bdl
CaO	bdl	0.90	bdl	bdl	0.28	bdl	0.07	bdl	0.10	0.31	0.45	0.56
Na_2O	1.50	1.25	1.18	1.12	0.81	0.96	1.06	1.01	15.16	15.39	16.03	15.97
K_2O	28.97	28.08	27.86	27.74	27.37	28.91	28.58	28.99	8.78	8.34	7.24	7.29
Total	99.77	100.32	99.96	100.41	100.28	100.26	99.83	100.39	98.83	99.15	100.84	100.38
Number of ions on the basis of 32 O												
Si	7.999	8.045	8.195	8.198	8.032	7.981	7.984	7.978	8.274	8.036	8.219	8.202
Al	7.055	7.146	7.169	7.264	7.731	7.678	7.679	7.714	6.974	6.673	7.395	7.443
Fe^{3+}	1.661	1.336	1.082	1.002	0.580	0.486	0.453	0.413	1.311	2.693	0.609	0.487
Mg	-	-	0.075	0.046	-	0.013	0.015	-	-	-	-	-
Ca	-	0.202	-	-	0.062	-	0.016	-	0.021	0.065	0.092	0.116
Na	0.615	0.507	0.477	0.450	0.325	0.392	0.431	0.409	5.790	5.858	5.957	5.969
K	7.816	7.492	7.410	7.331	7.229	7.735	7.679	7.749	2.206	2.089	1.770	1.793
Sum	25.146	24.728	24.408	24.291	23.959	24.284	24.257	24.263	24.577	25.415	24.042	24.010

* Total iron. bdl – below detection limits (0.04 wt.%).

TABLE 6

Representative analyses of haüyne and feldspar

	Haüyne					Feldspar			
location	PS 1	PS 2	PS 3	AH/25 4	AH/25 5	*location*	CF 1	CF 2	CF 3
SiO_2	31.92	36.25	35.72	31.02	31.33	SiO_2	45.76	43.60	44.18
Al_2O_3	27.14	29.22	28.45	26.19	26.31	TiO_2	bdl	bdl	bdl
Fe_2O_3*	0.46	0.84	1.97	0.30	0.32	Al_2O_3	33.26	35.40	35.16
MgO	bdl	0.13	bdl	0.15	0.17	MgO	0.29	bdl	bdl
CaO	6.15	1.29	1.25	9.23	9.21	CaO	18.15	19.33	18.93
Na_2O	13.44	21.57	19.08	7.91	8.11	Fe_2O_3*	1.22	0.96	0.81
K_2O	4.99	3.04	2.70	5.15	5.34	Na_2O	0.82	0.31	0.39
SrO	bdl	0.07	bdl	0.24	bdl	K_2O	0.34	0.25	0.39
BaO	0.50	0.12	bdl	0.04	0.13	Total	99.91	99.85	99.86
Cl	0.99	6.08	5.38	0.29	0.28				
SO_3	10.72	1.71	4.32	11.47	11.89	**Number of ions on the basis of 32O**			
Total	96.31	100.31	98.87	91.97	93.08	Si	8.481	8.110	8.203
O=Cl	0.23	4.71	1.24	0.22	0.22	Ti	-	-	-
Total	96.08	95.61	97.63	91.74	92.87	Al	7.266	7.761	7.694
						Mg	0.079	-	-
Number of ions on the basis of 21 O						Ca	3.605	3.852	3.766
Si	4.362	4.879	4.802	4.372	4.359	Fe^{3+}	0.255	0.201	0.170
Al	4.573	4.850	4.717	4.551	4.515	Na	0.296	0.112	0.140
Fe^{3+}	0.049	0.089	0.208	0.033	0.035	K	0.080	0.059	0.092
Mg	-	0.028	-	0.033	0.037	Sum	20.071	20.095	20.066
Ca	0.941	0.194	0.188	1.457	1.435				
Na	3.723	5.883	5.200	2.259	2.286	Z	16.01	16.07	16.07
K	0.910	0.546	0.484	0.969	0.990	Y	-	-	-
Sr	0.000	0.006	-	0.021	-	X	3.99	4.02	4.00
Ba	0.028	0.007	-	0.002	0.008				
Cl	0.240	1.449	1.282	0.072	0.069	Or	2.0	1.5	2.3
SO_3	1.148	0.180	0.455	1.267	1.297	Ab	7.4	2.8	3.5
Sum	15.974	18.110	17.336	15.034	15.031	An	90.5	95.7	94.2

* Total iron. bdl – below detection limits (0.04 wt.%).

that Italian melilitolites formed at very shallow depths.

Nepheline occurs both in PS and SV rocks as a groundmass phase or as inclusions in melilite. Only scanty nepheline compositional data are available (Table 5).

Kalsilite is typical of IUP kamafugites and has been identified in small amounts in most IUP melilitites, including a Vulture occurrence (Cinquini, 1999), but it may not be considered an essential constituent of IUP melilitolites, excluding the SV occurrence, where kalsilite was estimated at 6.5 modal %. Instead, RR ejecta contain essential (8.8 vol%) to dominant (35.5vol%) kalsilite (Table 1). IUP kalsilite is characterised by a higher Si/Al ratio than that of kalsilite from RR xenoliths, which has a higher [Al+Fe^{3+}] in the structural formula (Table 5). The ratio [Al+Fe^{3+}/Na+K+2Ca] is =1, while this ratio for IUP nephelines from

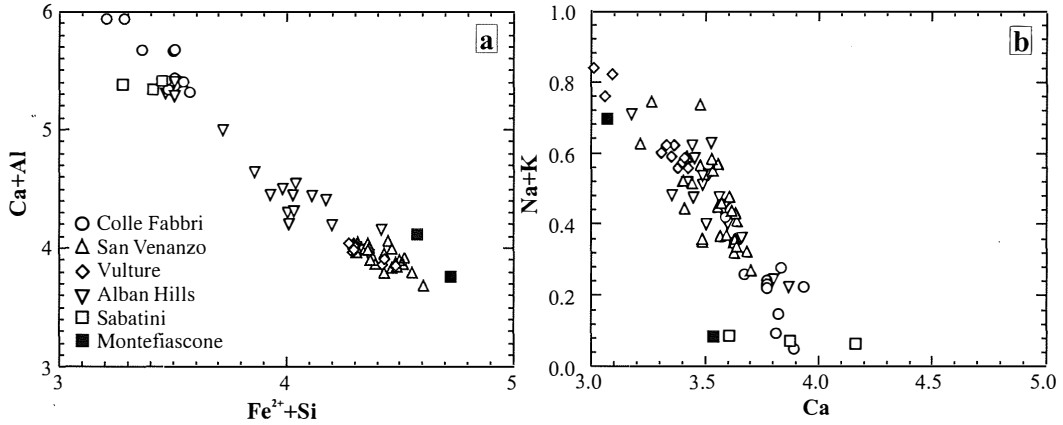

Fig 4 a and b – Melilite trends in ters of Ca + Al vs Fe + Si and Ca vs alkali for IUP melilitolites and RR ejecta.

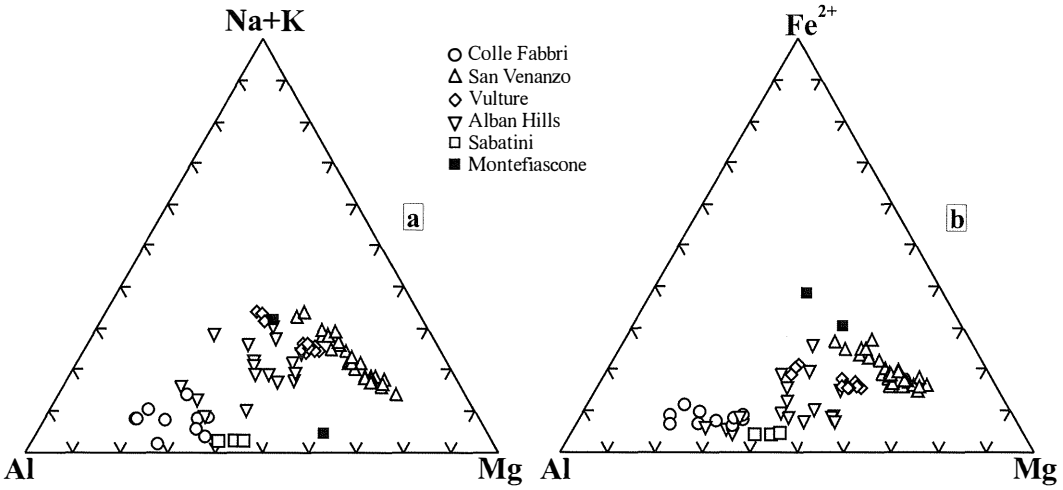

Fig. 5. a and b – melilite relationships in term of (Na+K)-Al-Mg and Fe-Al-Mg among and between IUP melilitolites and RR ejecta, respectively.

melilitolite is lower, reflecting a higher Agpaitic Index [=(K+Na/Al)] of the leucite melilitolite crystallizing liquid (Fig. 6a). The Na_2O/K_2O ratios of SV leucite melilitolite cluster around San Venanzo melilitite compositions (Figs 6a and b). Kalsilite is a crucial mineral in the kamafugite classification. However, it should be noted that not all the rocks which contain kalsilite are kamafugites.

Haüyne and nosean occur both as phenocrystal and groundmass constituents. PS samples contain essential nosean (10vol%), while haüyne typically occurs in RR meliltolites but in smaller amounts (up to 2 vol%).

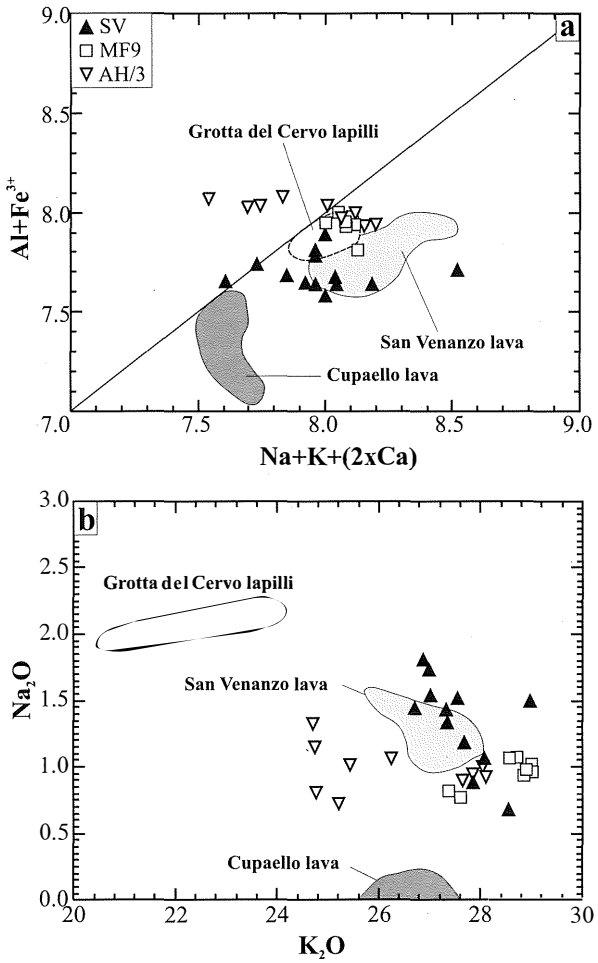

Fig. 6 – Kalsilite compositions of IUP melilitolites, RR ejecta and IUP melilitites in term of Al, Fe and alkalis.

BULK-ROCK GEOCHEMISTRY

Selected major, trace and isotopic compositions of IUP leucite melilitites are given in Table 11. CF has a similar SiO_2 wt% compared with that of other Italian melilitolites (mean SiO_2=41.9%wt and 100xQ/Si= -33.4) with a 100xK/Alk averaging 73. This rock is chemically a kamafugite according to Sahama's (1974) criteria. Its K_2O/Na_2O ratio (2.8) is very similar to that of the IUP melilitites, but low alkali (mean K_2O+Na_2O=1.67%wt), suggests that these elements may be lost during foids crystallisation, but after crystallisation of wollastonite and melilitite, because the latter constituents incorporate high-K melts in glass inclusions and leucite-kalsilite intergrowths (Table 6).

CaO is extremely high and averages (mean) 37.8%wt. Similar values are typical of silico-carbonatites and carbonatites but, among silicate rocks, are only known from intrusive rocks such as melilitolites (uncompahgrite) and

TABLE 7

Representative analyses of olivine

	SV 1	SV 2	MF5 3	MF5 4	MF5 5	AH/26 6	AH/26 7
SiO_2	41.40	40.31	36.93	40.83	35.15	40.67	41.17
FeO*	8.39	16.72	28.65	8.93	37.69	6.95	6.89
MnO	bdl	0.49	0.80	0.24	1.28	0.64	0.61
MgO	49.99	40.90	32.54	49.06	25.45	50.51	50.77
CaO	0.23	1.58	0.65	0.47	0.49	0.72	0.75
NiO	bdl	bdl	0.09	0.33	0.10	bdl	bdl
Total	100.01	100.00	99.65	99.86	100.16	99.49	100.20
Number of ionson the basis of 4 O							
Si	1.006	1.023	0.999	1.001	0.993	0.993	0.997
Fe^{+2}	0.171	0.355	0.649	0.183	0.891	0.142	0.140
Mn	0.000	0.011	0.018	0.005	0.031	0.013	0.012
Mg	1.811	1.547	1.313	1.792	1.072	1.838	1.833
Ca	0.006	0.043	0.019	0.012	0.015	0.019	0.019
Ni	-	-	0.002	0.007	0.002	-	-
Sum	2.994	2.977	3.000	2.999	3.004	3.005	3.002
Mg#	0.91	0.81	0.67	0.91	0.55	0.93	0.93

* total iron. bdl – below detection limits (0.04 wt.%)

TABLE 8

Representative analyses of phlogopite

location	SV 1	SV 2	MF9 3	AH/26 4	AH/26 5	AH/26 6
SiO_2	40.04	37.29	36.25	36.68	36.94	36.73
TiO_2	2.40	3.36	1.59	0.65	0.67	0.64
Al_2O_3	10.79	11.92	13.63	18.28	18.07	17.79
FeO*	5.13	6.16	16.93	3.59	3.49	2.86
MnO	0.10	0.11	0.49	0.09	0.05	0.06
MgO	22.24	19.79	14.49	23.15	23.17	23.88
CaO	0.22	0.10	1.56	0.08	0.08	bdl
Na_2O	0.20	0.18	0.69	0.13	0.18	0.13
K_2O	9.93	9.20	9.34	10.57	10.52	10.51
BaO	1.03	2.14	0.67	0.15	0.26	0.64
F	5.46	4.47	bdl	bdl	bdl	bdl
Total	97.54	94.72	95.64	93.42	93.47	93.34
Number of ions on the basis of 22 O						
Si	5.974	5.759	5.549	5.333	5.365	5.347
Ti	0.269	0.390	0.191	0.075	0.076	0.073
Al	1.878	2.148	2.573	3.278	3.237	3.193
Fe^{2+}	0.640	0.796	2.266	0.456	0.443	0.363
Mn	0.013	0.014	0.066	0.012	0.006	0.008
Mg	4.947	4.557	3.456	5.243	5.243	5.417
Ca	0.035	0.017	0.267	0.013	0.013	-
Na	0.058	0.054	0.214	0.039	0.054	0.037
K	1.890	1.813	1.907	2.050	2.037	2.041
Ba	0.060	0.130	0.042	0.009	0.015	0.038
Sum	15.763	15.677	16.531	16.506	16.490	16.519
Mg#	0.89	0.85	0.60	0.92	0.92	0.94

*Total iron. bdl – below detection limits (0.04 wt.%).

TABLE 9

Representative analyses of oxides

	AH/26	CF	MF5	SV	SV	PS	AS(1)
SiO_2	0.05	0.23	0.11	0.26	7.49	0.33	bdl
TiO_2	0.11	13.67	14.16	0.57	18.09	12.00	0.04
Al_2O_3	62.28	5.97	5.90	15.70	1.58	0.82	60.37
Fe_2O_3*	6.86	33.68	34.53	3.64	18.81	42.63	10.95
FeO	5.89	43.27	40.45	12.28	42.43	38.38	5.80
MgO	23.05	0.60	2.34	14.72	10.32	1.18	23.28
MnO	0.37	0.73	0.82	bdl	0.88	1.61	0.20
CaO	bdl	bdl	bdl	bdl	0.74	0.14	0.07
Cr_2O_3	bdl	bdl	bdl	51.06	bdl	0.29	bdl
V_2O_3	bdl	1.15	bdl	bdl	0.43	bdl	bdl
Total	98.61	99.30	98.31	98.23	100.77	97.38	100.71
Number of ionson the basis of 4 O							
Si	0.001	0.008	0.004	0.008	0.280	0.013	-
Ti	0.002	0.378	0.391	0.014	0.449	0.347	0.001
Al	1.862	0.259	0.255	0.587	0.061	0.037	1.791
Fe^{3+}	0.131	0.933	0.954	0.087	0.468	1.234	0.207
Fe^{2+}	0.125	1.332	1.242	0.326	1.172	1.235	0.122
Mg	0.871	0.033	0.128	0.696	0.508	0.068	0.873
Mn	0.008	0.023	0.025	-	0.025	0.052	0.004
Ca	-	-	-	-	0.026	0.006	0.002
Cr	-	-	-	1.281	-	0.009	-
V	-	0.034	-	-	0.011	-	-
Sum	3.000	3.000	3.000	3.000	3.000	3.000	3.000
*End members***							
Spi	87.2	3.3	12.8	29.4	3.1	1.9	87.5
Her	5.9	9.7	-	-	-	-	2.0
Qua	-	-	0.0	2.2	25.2	2.7	-
Mfe	-	-	-	4.4	-	-	-
Cou	-	1.7	-	-	0.6	-	-
Jac	0.8	2.3	2.5	-	2.5	5.2	0.4
Usp	0.3	38.7	39.5	-	47.8	33.3	0.1
Mnc	-	-	-	-	-	-	-
Pic	-	-	-	31.6	-	-	-
Chr	-	-	-	32.5	-	0.4	-
Mag	5.8	44.4	45.2	-	20.9	56.5	9.9
Sum	100.0	100.0	100.0	100.0	100.0	100.0	100.0

*Fe^{3+} recalculated after Droop (1987). (1) – average of 3 analyses. dl = below detection limit estimated as 0.05 wt.%. ** Endmembers recalculation after Stormer (1983).

ultramafic lamprophyres (wollastonite alnöite). Wollastonite is undoubtedly a liquidus phase in some of these rocks. Even more extreme Ca-silicates such as cuspidine and götzenite have been shown to have crystallised from the SV leucite melilitolite liquid (Sharygin *et al.*, 1996)

Mg# values of 60-70 suggest that CF may still represent a near-primary mantle melt.

TABLE 10

Representative analyses of perovskite.

	1	2	3	4	4
SiO_2	1.12	0.06	0.04	bdl	0.06
TiO_2	12.40	52.03	9.93	13.12	52.22
ZrO_2	bdl	bdl	0.11	bdl	bdl
HfO_2	bdl	bdl	0.13	0.18	bdl
ThO_2	0.05	0.57	bdl	bdl	0.56
UO_2	bdl	bdl	0.13	bdl	bdl
WO_3	0.07	0.09	bdl	0.10	bdl
Nb_2O_5	bdl	0.74	0.08	bdl	0.56
Ta_2O_5	0.04	0.13	0.06	0.09	0.15
Al_2O_3	1.48	0.42	0.84	1.04	0.38
Y_2O_3	bdl	0.06	bdl	bdl	0.05
La_2O_3	<0.05	1.10	<0.05	<0.05	0.91
Ce_2O_3	<0.05	3.30	<0.05	<0.05	2.71
Pr_2O_3	<0.2	0.44	<0.2	<0.2	0.36
Nd_2O_3	<0.1	1.44	<0.1	<0.1	1.16
MgO	1.27	bdl	0.71	1.69	0.00
CaO	0.42	35.08	0.11	0.04	36.47
MnO	1.52	0.07	1.45	1.50	0.02
FeO*	74.47	1.96	79.11	76.09	2.06
SrO	0.07	0.39	bdl	bdl	0.38
BaO	0.19	0.45	0.10	0.18	0.44
PbO	0.12	bdl	bdl	bdl	bdl
Na_2O	0.06	0.63	0.03	0.07	0.34
K_2O	0.07	0.04	0.08	0.04	0.06
F	0.05	0.09	0.04	bdl	bdl
Total	93.46	99.08	92.98	94.23	98.90

* Total iron. bdl – below detection limits (0.04 wt.%).

However, relatively low Cr and Ni, averaging (mean) 97 and 43 ppm, respectively, and absence of olivine suggest that CF may have undergone substantial crystal fractionation. Alternatively, a peculiar mantle composition may have been involved.

Mantle-normalized incompatible element patterns, show that CF conforms to the established patterns for regionally associated IUP rocks, but at lower concentration levels (Fig. 7a, Table 11). $[REE]_{CN}$ show the lowest values among IUP melilitites and melilitolites (Fig. 7b). La/Yb =c.16. This is interpreted to reflect depletion of CO_2 and/or removal of a carbonatite fraction, with relative depletion of LREE and HFSE, which are not easily accommodated in melilite, wollastonite and foids. A possible contribution from Ti-schorlomite in enhancing HREE remains unevaluated. Therefore, it is inferred that most hydromagmatophile elements initially present in the parental melt were lost during CF magma emplacement. In fact, the CF mineral assemblage is extremely dry and high temperature based on melilite-wollastonite-leucite equilibrium(c.1280°C). The high concentration of K-Ba-bearing minerals found in the surrounding rocks indicates substantial metasomatic effects and magma elemental loss (Wheeler *et al.*, 1996). These processes would have been favoured by slow magma emplacement at shallow depths.

SV gives the lowest SiO_2 values (mean SiO_2=38.5%wt, 100x-Q/Si=-64.1) among Italian melilitolites. However, mean 100xK/Alk is 71.2, a value very similar to the CF analogue. This rock is chemically a kamafugite. The Mg# (mean=64) value is slightly lower, compared with the value for CF. Cr and Ni, mean 57 and 31 ppm, respectively, are also lower than the CF analogues. CaO is constant in spite of a clear inverse correlation between SiO_2 and CO_2, supporting the hypothesis that $CaCO_3 \rightarrow CaO + CO_2$.

SV also shows the highest LILE relative to other IUP melilitolites. HFSE are higher with respect to those for CF, but show very similar abundances to the PS analogues (Fig. 7a). REE are also high and show a marked Eu anomaly (Fig. 7b). La/Yb = c. 30. It is noteworthy that most trace elements are concentrated in a secondary mineral association which is very similar to that for CF (Wheeler, *et al.*, 1996; Capitanio and Wheeler, in press).

PS yielded SiO_2 concentrations similar to, or slightly lower than, those for CF, averaging (mean) 40.3%wt; mean 100x-Q/Si is -61. Total alkali are high (mean= 8.6%wt), while the K_2O/Na_2O and 100xK/Alk ratios are the lowest among Italian melilitolites (mean=1.05 and 41, respectively). Chemically, this rock may not be a kamafugite *sensu stricto* as it shows a

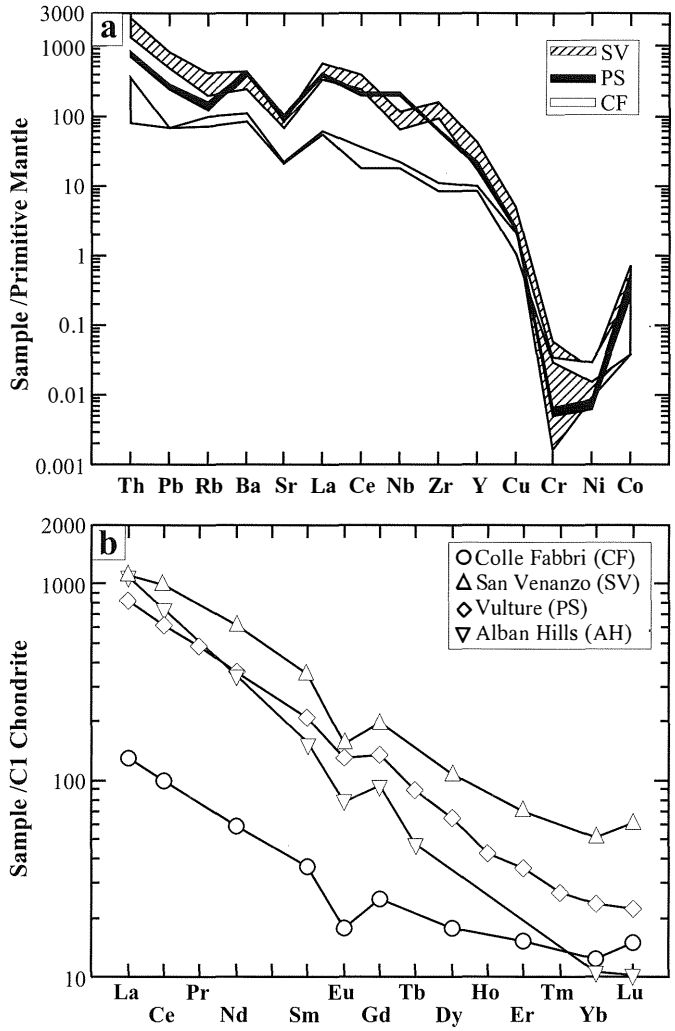

Fig. 7 – a: Mantle-normalized multi-element diagram for IUP melilitolites. b: $[REE]_{CN}$ diagram for IUP melilitolites and a AH ejectum (kalsilitolite).

relatively low K/Alk, which reflects absence of kalsilite. (K+Na)/Al values are relatively low (mean 0.82) and slightly lower than that for SV. CO_2 correlates positively with CaO and negatively with SiO_2. CaO (mean= 15.9%wt) is slightly lower than that for SV, i.e.17.7%wt and about half that for CF (37.8). Low Cr and Ni (17 and 15 ppm, respectively) and lower Mg# (55) indicate a higher fractionation degree, relative to more primitive IUP melilitolites. However, all melilitolites yielded lower Mg# relative to the associated melilitites and their parental liquid is residual with respect to the initial melilititic melt.

Mantle normalised trace element abundances show intermediate LILE, high HFSE and a distinctive Nb (Ta-Hf) positive anomaly with respect to other IUP melilitolites. These elements

TABLE 11

Analyses of major, trace including rare earths elements (REE).

sample	**PS**		**CF**		**SV**		**KTL**[1]
average of	6	*St Dev*	5	*St Dev*	7	*St Dev*	
SiO_2	40.29	*0.73*	41.89	*0.50*	38.11	*2.02*	42.54
TiO_2	2.04	*0.08*	0.37	*0.12*	2.24	*0.34*	0.78
Al_2O_3	14.30	*0.41*	10.70	*0.45*	9.53	*0.76*	12.84
Fe_2O_3	4.65	*0.88*	1.44	*0.36*	3.50	*0.61*	5.15
FeO	5.37	*0.28*	1.77	*0.27*	7.44	*0.91*	2.56
MnO	0.25	*0.01*	0.06	*0.01*	0.16	*0.06*	0.20
MgO	3.73	*0.18*	1.78	*0.08*	8.55	*1.53*	7.73
CaO	15.89	*0.42*	37.85	*0.76*	17.67	*0.53*	16.37
Na_2O	4.23	*0.42*	0.45	*0.09*	1.43	*0.37*	1.13
K_2O	4.39	*0.22*	1.22	*0.11*	5.93	*0.60*	9.13
P_2O_5	1.02	*0.02*	0.15	*0.02*	1.22	*0.15*	0.71
CO_2	0.47	*0.15*	0.04	*0.09*	1.32	*1.70*	0.00
LOI	2.62	*0.55*	1.41	*0.92*	2.76	*1.95*	1.05
Total	99.24		99.12		99.86		100.19
Trace elements (ppm)							
V	240.1	*117.0*	97.8	*3.8*	436.7	*76.6*	nd
Sc	nd		13.6	*0.7*	15.8	*38.7*	26.8
Cr	17.1	*1.6*	96.8	*7.9*	57.2	*64.8*	233.0
Co	43.1	*10.3*	6.0	*2.2*	34.3	*27.8*	34.0
Ni	14.9	*1.8*	42.8	*12.7*	31.0	*12.4*	90.0
Cu	70.5	*2.1*	33.0	*2.9*	109.6	*31.1*	nd
Zn	176.9	*4.1*	70.8	*15.3*	90.1	*7.2*	nd
Ga	21.8	*1.9*	22.5	*1.7*	21.1	*4.2*	nd
Rb	108.4	*10.0*	58.8	*5.3*	210.2	*57.9*	256.0
Sr	2666.3	*97.3*	584.3	*9.9*	2169.0	*144.5*	1659.0
Y	184.2	*283.9*	32.0	*1.4*	101.8	*31.1*	25.0
Zr	518.4	*10.9*	77.3	*6.1*	1085.8	*209.9*	328.0
Nb	117.9	*3.9*	10.8	*1.0*	54.3	*12.8*	nd
Ba	2353.4	*85.8*	526.5	*70.7*	2009.5	*399.9*	997.0
Pb	31.3	*2.2*	nd		56.1	*45.9*	nd
Th	48.8	*3.2*	21.5	*1.3*	136.1	*28.6*	69.0
REE (ppm)							
La	208.3	*8.9*	30.0	*1.6*	249.7	*39.0*	259.0
Ce	348.7	*16.1*	56.3	*4.3*	566.3	*90.5*	455.0
Nd	166.8		27.2	*2.9*	285.1	*0.1*	160.0
Sm	31.9		5.4	*0.2*	53.1	*0.1*	24.1
Eu	7.5		1.0	*0.0*	9.0		4.5
Gd	27.6		4.9	*0.3*	40.3		19.4
Dy	16.2		4.3	*0.2*	27.4		nd
Er	5.9		3.2	*1.6*	11.6		nd
Yb	4.0		2.0	*0.1*	8.7		1.8
Lu	0.6		0.4	*0.0*	1.5		0.3
Isotopic ratios							
$^{87}Sr/^{86}Sr$	0.706325		0.709702		0.710571		0.71036
$^{143}Nd/^{144}Nd$	0.512613		0.512068		0.512091		0.51186

[1] data from Federico *et al.*, (1994). nd – not determined.

are mostly concentrated in perovskite (Table 10). REE patterns show the highest fractionation of LREE/HREE among IUP melilitolites and only a slight Eu anomaly (Fig. 7b).

A few bulk rock data are available for the RR ejecta, in which the association of kalsilite plus essential melilite, i.e. the main mineralogical indicators of kamafugites, has not been recognised. Extremely variable mineralogy and field occurrence indicate a wide compositional spectrum which requires a systematic study. However, an exhaustive and detailed description of the different types of RR ejecta is beyond the aim of this paper and only a sample from the Alban Hills is considered to approach the kamafugitic composition (Federico *et al.*, 1994). This sample, AH/3 has a slightly higher SiO_2 (41.9wt%) with respect to IUP melilitolites, higher alkali (10.3wt%), K_2O/Na_2O = 8.1 and 100xK/Alk = 0.84. However, CaO and the (K+Na)/Al ratio are consistent with those for IUP melilitolites. Ni, Cr and Mg# are higher (Fig. 8a). Most of the trace elements are comparable with those for IUP melilitolites, but Sr/Ba is much higher (Fig. 8b). A Sr/Ba ratio of about 1 is considered characteristic of kamafugites (Fig. 8b), whereas higher values are characteristic of leucitites (Sahama, 1974). REE are much more fractionated and show 'cross-cutting' relationships with those for IUP melilitolites (Fig. 7b). This extreme LREE/HREE is not typical of IUP leucite melilitolites and may well be related to a distinct crystallization differentiation process. However, it seems entirely possible that this may be related to the low-pressure crustal regime, rather than source mantle and melt high-pressure evolution.

Melt inclusions

Melt inclusions were identified in the majority of SV silicate minerals. In larger crystals (melilite, olivine, leucite) these inclusions are mainly localized in the outer zones and are usually associated with fluid, polycrystal and combined polycrystal aggregate+adhered melt or fluid (Sharygin *et al.*, 1996; Stoppa *et al.*, 1997, Sharygin, 1999; Sharygin, 2001). The phenocryst-hosted inclusions yielded T_{hom} >>1025°C in olivine, T_{hom} =1180-1240°C in melilite, T_{hom} >1150°C in leucite. In the groundmass minerals (nepheline, kalsilite, apatite, cuspidine, clinopyroxene, phlogopite) the silicate-melt inclusions cluster in the crystal core. They consist of green or brown glass ± fluid bubble ± carbonate globule ± trapped/daughter crystals (pyrrhotite, clinopyroxene, kalsilite, westerveldite). Inclusions in kalsilite and nepheline yielded T_{hom}=830-870°C. The modal abundance of carbonate globules in silicate-melt inclusions suggests that widespread separation of carbonatite occurred at lower temperatures after crystallization of kalsilite (800°C) and textural evidence suggests carbonate and cuspidine co-precipitation during ocellar segregation (Sharygin *et al.*, 1996; Stoppa *et al.*, 1997) . The silicate glass melts at 560-620°C, and the carbonate globules begin to melt at 600-650°C. High concentrations of B_2O_3 and FeO in the residual silicate melt decreased its solidus temperature (Sharygin, 1999). This probably prompted complete fluid separation from the carbonatitic liquid.

Trapped glass inclusions were found in CF wollastonite. They have high K_2O (c. 7.0 wt.%) and (Na+K)/Al = 0.9, which reflect the initial near peralkaline nature of the liquid.

Significance of IUP Leucite Melilitolite Paragenesis

The initial melilitolite melt probably represents a residual melilititic-kamafugitic liquid enriched in CaO and alkali and depleted in Al_2O_3 (agpaitic index > 0.9). These conditions allowed further crystallization of calcium silicates such as cuspidine (mean CaO=39.4 wt%), götzenite (mean CaO=53.2wt%), wollastonite (mean CaO=45.8wt%). Therefore, the IUP melilitolites yield the most Ca-rich compositions of the kamafugite association in

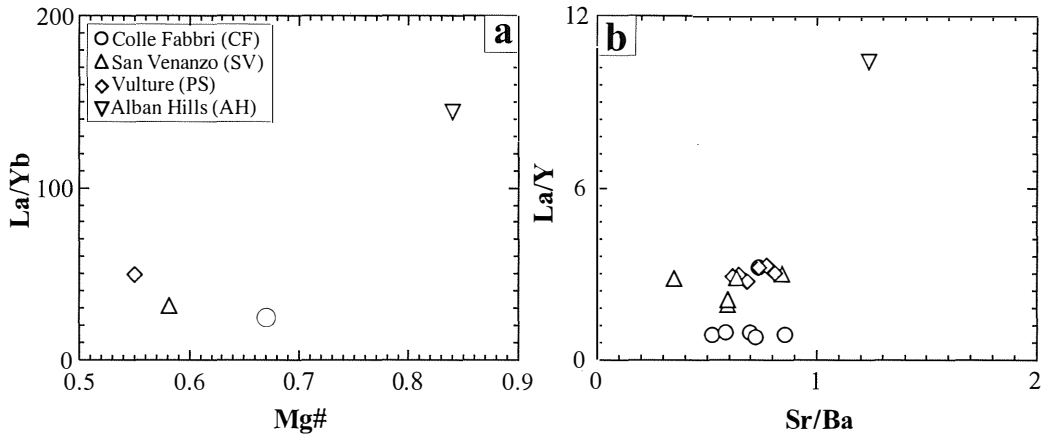

Fig. 8 – a and b: Main compositional differences between IUP melilitolites and 'kamafugitic' kalsilitolite ejecta from the Alban Hills (Federico *et al.*, 1994)

Italy, and their extreme Ca-enrichment is a crucial petrogenetic factor.

A high CaO content prompted two important results. The first is the appearance of modal wollastonite, expected in the leucite-wollastonite-melilite plane of the kalsilite –wollastonite- diopside - åkermanite system, i.e. Yoder's (1973) sub-tetrahedron, in which all the Italian melilitolites may be projected. Also, crystallization in the system leucite-åkermanite-SiO_2, ignoring the small contribution of Al to diopside and melilite, is essentially controlled by the joins Lc-(Di+Wo) and Sa-(Di+Wo) (Gupta and Gupta, 1997), leading to an assemblage of wollastonite-melilite leucitite at T=1280°C under atmospheric pressure, closely approaching that of the CF rock. This supports the view that crystal-liquid equilibrium in the CF silicate melt, possibly modified by a carbonatite component, generated a stable high temperature mineral assemblage.

The second important result is the possible production of modal carbonate. In fact, the IUP melilitolites preserved some carbonate as globules, ocelli, and patches in the groundmass, which are presumed to have formed by immiscibility at relatively low temperatures (670-800°C) and low pressure (<1 kb). However, carbonate immiscibility should not be dominant in melilitolite genesis as the factors which favour crystallization of Ca-rich silicates probably prevent abundant separation of carbonatitic liquid at higher temperatures, at which melilite, wollastonite and Ti-Zr-garnet are stable (>1050°C).

These two results are both consistent with the IUP leucite melilitolite assemblages, in which the $CaCO_3 = CaO + CO_2$ reaction dominates the higher temperature–low pressure regime. On the other hands, immiscibility is expected to occur only at lower temperatures (<800°C) when volatile concentration depresses the silicate melt solidus temperature, the condition pertaining at SV, as indicated experimentally and by textural relationships. At this stage Ca-silicates cannot accommodate substantial incompatible elements (LILE), which are further concentrated in the residual liquid, which attained a strongly peralkaline composition (SV and CF), or were dispersed, depending on geological conditions, through the enclosing rocks (CF).

The IUP regional association of primary calciocarbonatites and olivine melilitites or kamafugites is dominated by high temperature and high pressure immiscibility of a carbonatite fraction from kamafugite (Stoppa *et al.*, 2003a). Further reaction of phlogopite and olivine, under the crustal pressure regime

and high temperature, may account for the generation of clinopyroxene, melilite and leucite/kalsilite, but not wollastonite, götzenite, cuspidine, monticellite and anorthite. On the other hand, if carbonatite-silicate liquid immiscibility is the dominant process at high temperatures and pressures (conjugate carbonatite and melilitite eruption), miaskitic residual liquids may result by this process as carbonate cannot accommodate Al_2O_3.

Mantle olivine (Fo_{97}) from San Venanzo (Pian di Celle) kamafugites contains high-temperature (T>1360°C) melt inclusions, corresponding in composition to alkaline clinopyroxenite (Panina *et al.*, 2003). This confirms the evolution trends delineated and discussed in Stoppa and Cundari (1998, in Fig. 5) and rules out any hypothesis involving forsterite forming by magmatic reaction with dolomite country rocks (Peccerillo, 1998). A trend of progressive melt SiO_2-undersaturation from basanite differentiation or dolomite assimilation by basanitic magma is inconsistent with the composition of the residual kamafugite glass, which trends toward SiO_2-saturation (Stoppa and Cundari, 1998). This is confirmed by lower temperature fluid inclusions in SV and CF melilitolites and in IUP melilitites in general. In the latter, the fluid inclusions show two distinct residual-glass trends, one towards hyper-agpaitic (IUP-like) melts with alkali enrichment and aluminium depletion (melilitolites); the other towards miaskitic compositions, rich in silica and alumina corresponding to the phonolitic tuffs present at San Venanzo and Cupaello as well as other IUP outcrops (Stoppa and Lavecchia, 1992; Stoppa and Cundari, 1998; Panina *et al.*, 2003).

Discussion

Based on stratigraphical and structural observations, IUP melilitolites represent a final event of the related volcanic activity, inferred to have occurred as a slow, sub-volcanic emplacement, which may represent the surface expression of larger intrusions at depth. The presence of volcanic breccias and fragmentation of the invaded country rocks, the latter notably at Colle Fabbri, associated with melilitolite intrusion is attributed to CO_2-driven, shallow explosive phenomena during melilitolite crystallization. Other indicators of volatile flow associated with the melilitolite bodies are represented by the ample thermal aureoles in the country rocks. Therefore, melilitolite development seems to be related to a low-velocity ascent of carbonatitic-kamafugitic magma after crystal settling and CO_2 accumulation and dispersal in the crustal T-P regime.

IUP melilitolites do not exhibit cumulus textures and represent *in situ* crystallisation of high temperature mafic alkaline melts. A large textural spectrum has been seen in RR ejecta. Some may be high pressure rocks or subvolcanics, others are cumulus rocks.

IUP leucite melilitolites and RR ejecta have distinct mineral chemistry, reflecting their initial peralkaline and metaluminous nature, respectively. This distinction is sharp for IUP melilitolites (Stoppa *et al.*, 2002), but is blurred for RR ejecta (Cundari and Salviulo, 1987; Federico *et al.*, 1994). This may be germane to the absence at the surface of a carbonatite component, non-essential modal melilite and essential feldspar/plagioclase in the Roman Region. Also, IUP clinopyroxene, olivine and leucite coexisting with essential melilite are enriched in Ca and depleted in Si, relative to their analogues in the RR ejecta. Clinopyroxene, high Ti, Zr garnets, and especially apatite and perovskite coexisting with essential melilite and in the absence of melilite, respectively, are characterized by different site occupancies, reflecting the distinct Sr, Ba, REE, and Zr of the host rock compositions (Stoppa *et al.*, 2002).

The presence of miaskitic and peralkaline assemblages parallels the regional association of two rock suites, kamafugites and plagio-leucitites, described in several continental grabens world-wide, where coeval carbonatite

may also occur (e.g. Stoppa and Woolley, 1997; Bailey and Collier, 2000; Stoppa *et al.*, 2003b). Alternatively, some petrologists have adopted the *a priori* view that the two associations are co-genetic and derived from a common parental leucitite and/or basanite liquid, with the melilite-bearing compositions being fractionated from the latter (e.g. Melluso *et al.*, 1996; Bindi *et al.*, 1999, Beccaluva *et al.*, 2002) or produced by assimilation of sedimentary rocks (Peccerillo, 1998).

Assuming consanguinity and differentiation of late-stage leucite-melilitolite assemblages from parental leucitite/basanite, as suggested by Melluso *et al.* (1996) and Bindi *et al.* (1999), an essential Ca increase and Al decrease by means of crystallization differentiation remains unaccounted for. Sediment(s) assimilation by magma to match the desired target composition would be strongly endothermic and would tend to freeze the hypothetical 'hybrid' magma. In addition, sediment assimilation is ruled out by Sr-Nd isotope geochemistry and trace element mass balance, distribution of REE and melt inclusion studies (Castorina *et al.*, 2000; Panina, 2003; Stoppa, 2003). Therefore, this hypothesis is not supported by specific petrological and geological evidence.

The crystallization sequence of melilite-bearing assemblages may lead both to IUP leucite melilitolite or to RR kalsilite-clinopyroxenite compositions, depending on fractionation and/or reactions of the type Ol+Phl = Mel+Lc+Ks = Cpx+Lc+Ks (Cundari and Ferguson, 1991; Stoppa *et al.*, 1997; Stoppa *et al.*, 2002). However, the compositions of the IUP rock associations and RR ejecta, projected in de la Roche's R1-Rm-Rs diagram and other semi-modal diagrams, clearly demonstrate that the resulting trends could not be assigned to the same parental magma and that a possible parental composition with relatively high Ca and REE, similar to carbonatite, is indicated (Fig. 13 in Stoppa *et al.*, 2002).

SUMMARY AND CONCLUSIONS

Several lines of evidence, based on the nature of the lithosphere, experimental data, detailed geochemistry and mineral chemistry, consistently support the view that the IUP and the RR series originated from distinct primary and/or near-primary magmas from different mantle regions and occupy different, even if conjugate, tectonic settings. High-pressure CO_2 exolution (diatresis) would explain mantle breccia and tuffisite formation, which are typical of carbonatite-kamafugite extrusives (Stoppa *et al.*, 2003). Melilitolite formation is a relatively rare variant of this mechanisms in which CaO is retained in the silicate fraction by $CaCO_3$ decoupling and CO_2 exolution at high temperature and low pressure. However, melilitolites are relatively evolved rocks and cannot represent the primary silico-carbonatitic magma of IUP.

Complete or partial separation of the coexisting carbonatite from the melilititic silicate fraction may occur under pressures higher than those for the melilite stability field (less than 14 kbar; Yoder, 1973). The occurrence of IUP conjugate eruption of Ca-carbonatite and kamafugite in chemical equilibrium, is undoubtedly related to carbonate-silicate immiscibility which most probably occurred under deep-seated conditions at temperatures higher than 1300°C (Panina *et al.*, 2003; Stoppa and Lloyd, 2003). Thereafter, carbonatite may have reached the surface as a distinct explosive eruption, forming the carbonatite facies, while the same primary mantle melt may have evolved to form kamafugites, melilitolites and peralkaline phonolites. This may well be the case for the Polino and Oricola carbonatites and nearby melilitite occurrences at San Venanzo and Cupaello, which contain significant carbonate or discrete carbonatites (Stoppa and Woolley, 1997).

A liquidus temperature determined at atmospheric pressure for kamafugitic melilitites yielded 1270°C (Cundari and Ferguson 1991). This is consistent with

experimantal crystallization in the system leucite-åkermanite-SiO_2. Ignoring the small contribution of Al to diopside and melilite, respectively, crystallization is controlled by the joins Lc-(Di+Wo) as well as Sa-(Di+Wo) (Gupta and Yagi, 1997) leading to an assemblage of wollastonite-melilite leucitite at T=1280°C under atmospheric pressure, closely approaching that of the CF rock. Notably, the liquidus temperature of the parental magma was estimated at 1360 °C by melt inclusions in high pressure minerals (Panina *et al.*, 2003).

Further, significant results have been obtained from the study of melt inclusions and residual glasses in Italian melilitites and melilitolites (Stoppa *et al.*, 1997; Stoppa and Cundari, 1998; Sharigin, 1999; Panina *et al.*, 2003) which confirm a possible evolution toward metaluminous phonolites as well as hyperalkaline phonolites. However, while melilitite magma *sensu lato* may not be parental to plagioclase-free leucitite magma, it appears to share some genetic features with the latter, as indicated by the occurrence of accessory melilite in RR ejecta. Also, metaluminous phonolitic residua may be derived from melilitite liquids, controlled by melilite and kalsilite reaction with the liquid to form leucite/sanidine (Cundari and Stoppa, 1998). This accounts for the transition from peralkaline liquids of melilitite and melilitolite composition to metaluminous phonolitic liquids within IUP, but may not necessarily apply to the genesis of the RR phonolites, which is beyond the scope of this paper.

Conditions necessary for diatresis, carbonate-silicate immiscibility and formation of perakaline rocks seem to occur in thick lithospheric structures, observed in the IUP area (Lavecchia and Boncio, 2000; Lavecchia and Creati, 2002). Therefore, olivine-melilitites and kamafugites may have originated from a deeper source, under a thicker lithosphere and lower heat flow, reflecting their close association with carbonatite, relative to the conditions which prevailed for the generation of the much more abundant plagio-leucitite compositions (Lavecchia and Stoppa, 1996; Bailey and Collier, 2000).

ACKNOWLEDGMENTS

We wish to thank John Spratt and Terry Williams for their help with the Electron Microprobe work at the Natural History Museum, London. F. Stoppa's visits at the Natural Histroy Museum and use of its analytical facilities were funded by the European Commission's Improving Human Potential (IHP) Programme. A Cundari is grateful to Geotrack International Melbourne, for support and cooperation.

REFERENCES

ALBRECT A. (1981) — *Mineralogische Untersuchung des Phonolites vom Fohberg, Kaiserstuhl.* Unpubl. Thesis. Univ. Freiburg, 137 pp.

AURISICCHIO C. and FEDERICO M. (1985) — *Nepheline-kalsilite microperthites in ejecta from the Alban Hills (Italy).* Bull. Soc. Geol. Finland **57**, 5-12

BAILEY D.K. and COLLIER J.D. (2000) — *Carbonatite-melilitite association in the Italian collision zone and the Ugandan rifted craton: significant common factors.* Mineral. Mag. **64**, 675-682.

BARKER D.S. and NIXON P.H. (1989) — *High-Ca, low-alkali carbonatite volcanism at Fort Portal, Uganda.* Contrib. Mineral. Petrol. **103**, 166-177.

BECCALUVA L., COLTORTI M., DI GIROLAMO P., MELLUSO L., DILANI L., MORRA V. and SIENA F. (2002) — *Petrogenisis and evolution of the Mt. Vulture alkaline volcanism (Southern Italy).* Mineral. Petrol., **74**, 277-297.

BELL K., CASTORINA F. and STOPPA F. (2001) — *Isotopic regional zoning versus tectonic polarity in Pleistocene leucitites, melilitites and carbonatites of the Italian peninsula.* EUGXI, J. Conf. Abst **6**, 495.

BINDI L., CELLAI, D., MELLUSO L., CONTICELLI S., MORRA V., and MENCHETTI S. (1999) — *Crystal chemistry of clinopyroxene from alkaline undersaturated rocks of the Mt Vulture Volcano, Italy.* Lithos **46**, 259-274.

CASTORINA F., STOPPA F., CUNDARI, A. and BARBIERI M. (2000) — *An enriched mantle source for Italy's melilitite-carbonatite association as inferred by its Nd-Sr isotope signature.* Mineral. Mag. **64**, 625-640.

CINQUINI N. (1999) — *Stratigraphy of Mt. Vulture.* Unpubl. Thesis. Univ. Pisa, 100 pp.

CUNDARI A. and FERGUSON A.K. (1991) — *Petrogenetic relationship between melilitite and lamproite in the Roman Region: the lavas of S. Venanzo and Cupaello.* Contrib. Mineral. Petrol. **107**, 343-357.

CUNDARI A and SALVIULO G. (1987) — *Clinopyroxene from Somma Vesuvio: implication of crystal chemistry and site configuration parameters for study of magma genesis.* J. Petrol. **28**, 727-736.

DI BATTISTINI G., MONTANINI A., VERNIA L., BARGOSSI G.M. and CASTORINA F. (1998) — *Petrology and geochemistry of ultrapotassic rocks from the Montefiascone Volcanix Complex (Central Italy): magmatic evolution and petrogenesis.* Lithos **43**, 169-195.

DROOP G.T.R. (1987) — *A general equation for estimating Fe^{3+} concentrations in ferromagnesian silicates and oxides from microprobe analyses, using stoichiometric criteria.* Mineral. Mag. **51**, 431-435.

DUNWORTH E.A. and BELL K. (1998) — *Melilitolites: a new scheme of classification.* Can. Mineral. **36**, 895-903.

FEDERICO M. and GIANFAGNA A. (1982) — *The melilites of the ejecta and lavas from the Alban Hills (Rome, Italy).* Rend. Soc. It. Mineral. Petrol. **38**, 1387-1400.

FEDERICO M., PECCERILLO A., BARBIERI M. and WU T.W. (1994) — *Mineralogical and geochemical study of granular xenoliths from the Alban Hills Volcano, Central Italy: bearing on evolutionary processes in potassic magma chambers.* Contrib. Mineral. Petrol. **115**, 384-401.

GALLO F., GIAMMETTI F., VENTURELLI G., and VERNIA L. (1984) — *The kamafugitic rocks of San Venanzo and Cupaello, Central Italy.* N. J. Mineral. Mon. **5**, 198-210.

GUPTA V.K. and GUPTA A.K. (1997) — *Phase relations in the system leucite – akermanite - albite – SiO_2 under one atmospheric pressure. Synthetic and natural rocks.* Yagi volume, Allied pub., 48-67

HOGARTH D.D. (1989) — *Pyrochlore, apatite, and amphibole: distinctive minerals in carbonatites.* In Carbonatites (K. Bell ed), Unwin Hyman, London, 105-141.

ITO J. and FRONDEL C. (1967) — *Syntetic and Titanium-garnets.* Am. Mineral. **52**, 7773-526.

LAVECCHIA G. and BONCIO P. (2000) — *Tectonic setting of the carbonatite-melilitite association of Italy.* Mineral. Mag. **64**, 583-592.

LAVECCHIA G. and CREATI N. (2002) — *The Intramontane ultra-alkaline Province (IUP) of Italy: a brief review with consideration on the thickness of the underling lithosphere.* Boll. Soc. Geol. It. **1**, 87-98.

LAVECCHIA G. and STOPPA F. (1996) — *The tectonic significance of Italian magmatism: an alternative view to the popular interpretation.* Terra Nova **8**, 435-446.

LUPINI L., WILLIAMS C.T. and WOOLLEY, A.R. (1992) — *Zr-rich garnet and Zr- and Th-rich perovskite from the Polino carbonatite, Italy.* Mineral. Mag. **56**, 581-586.

MELLUSO L., MORRA V. and DI GIROLAMO D. (1996) — *The Mt Vulture volcanic complex (Italy): evidence for distinct parental magmas and for residual melts with melilite.* Mineral. Petrol. **56**, 225-250.

PANINA L.I., STOPPA F., and USOLTSEVA L.M. (2003) — *Genesis of melilite rocks of the volcano Pian di Celli, from data of melt inclusion studies.* Russian J. Petrol. **4**, in press.

PECCERILLO A. (1998) — *Relationship between potassic and carbonate-rich volcanic rocks in central Italy: petrogenetic and geodynamic implications.* Lithos **43**, 267-279

SAHAMA T.G. (1974) — *Potassium rich alkaline rocks.* In Sorensen. H. (ed): The alkaline rocks. John Wiley & Sons, London, 96-109.

SCHINGARO E., SCORDARI F., CAPITANIO F., PARODI G., SMITH C.D. and MOTTANA A. (2001) — *Crystal chemistry of kimzeyite from Anguillar, Mts Sabatini, Italy.* Eur. J. Mineral. **13**, 749-759.

SHARYGIN V.V., STOPPA F., and KOLESOV B.A. (1996) — *Zr-Ti-disilicates from the Pian di Celle volcano, Umbria, Italy.* Eur. J. Mineral. **8**, 1199-1212.

SHARYGIN V.V. (1999) — *Boron-rich glasses in melilitolite from Pian di Celle, Umbria, Italy.* Terra Nostra **6**, 268-270.

SHARYGIN V.V. (2001) — *Silicate-carbonate liquid immiscibility in melt inclusions from melilitolite minerals: the Pian di Celle volcano (Umbria, Italy).* Memorias Universidade do Porto, Faculdade de Ciencias, Departamento de Geologia, Abstracts of XVI ECROFI, Porto, **7**, 399-402.

STOPPA F. (1988) — *L'Euremite di Colle Fabbri (Spoleto): un litotipo ad affinità carbonatitica in Italia.* Boll. Soc. Geol. **107**, 239-248.

STOPPA F. (2003) — *Consensus and open questions about Italian CO_2 – driven magma from the mantle.* Per. Mineral., this vol..

STOPPA F. and WOOLLEY A.R. (1997) — *The Italian carbonatites: field occurrence, petrology and regional significance.* Mineral Petrol **59**, 43-67.

STOPPA F. and CUNDARI A. (1995) — *A new Italian carbonatite occurrence at Cupaello (Rieti) and its genetic significance.* Contrib. Mineral. Petrol. **122**, 275-288.

STOPPA F. and CUNDARI A. (1998) — *Origin and multiple crystallization of the kamafugite-carbonatite association at S.Venanzo- Pian di Celle, Umbria, Italy.* Mineral. Mag. **62**, 273-289.

STOPPA F. and PRINCIPE C. (1998) — *High energy eruption of carbonatitic magma at Mt. Vulture (Southern Italy): the Monticchio Lakes Formation.* J. Volcanol. Geotherm. Res. **80**, 137-153.

STOPPA F. and LAVECCHIA G. (1992) — *Late Pleistocene ultra-alkaline magmatic activity in the Umbria-Latium region (Italy): an overview.* J. Volcanol. Geotherm. Res. **52**, 277-293.

STOPPA F., LLOYD F. and ROSATELLI G. (2003a) — *CO_2 as the virtual propellant of carbonatite-kamafugite conjugate pairs and the eruption of diatremic tuffisite.* Per. Mineral., this vol.

STOPPA F., ROSATELLI, G., WALL F. and LE BAS M.J. (2003b) — *Texture and mineralogy of tuffs and tuffisites at Ruri Volcano in western Kenya: a carbonatite, melilitite, mantle-debris trio.* Per. Mineral., this vol.

STOPPA F., SHARYGIN, V.V., and CUNDARI, A. (1997) — *New mineral data from the kamafugite-carbonatite association: the melilitolite from Pian di Celle, Italy.* Mineral. Petrol. **61**, 27-45.

STOPPA F., WOOLLEY A.R., and CUNDARI A. (2002) — *Extent of the central Appenine melilitite-carbonatite province: new evidence from kamafugite at Grotta del Cervo, Abbruzzo.* Mineral. Mag. **66**, 555-574.

STOPPANI F.S. and CURTI E. (1982) — *Minerali del Lazio.* Firenze. Editoriale Olimpia, pp 120.

WASHINGTON H.S. (1923) — *Italite: a new rocks.* Am. J. Sci. **51**, 33-42.

WHEELER S., SPIGARELLI S., STOPPA F., and RINALDI R. (1996) — *Secondary minerals from the igneous complex of Colle Fabbri, Spoleto (PG).* Plinius **16**, 211-212.

YODER H.S. (1975) — *Relationships of melilitite-bearing rocks to kimberlite: a preliminary report on the system Akermanite-CO_2.* Phys. Chem. Earth **9**, 883-894.

YODER H.S. (1973) — *Akermanite-CO_2: Relationships of melilite-bearing rocks to kimberlites.* Carnegie Institute, Geophysical Lab. **72**, 449-467.